

# Effect of cation-anion interactions on the structural and vibrational properties of 1-butyl-3-methyl imidazolium nitrate ionic liquid

Jonas Kausteklis<sup>a</sup>, Valdemaras Aleksa<sup>a</sup>, Maximiliano A. Iramain<sup>b</sup>,  
Silvia Antonia Brandán<sup>b,\*</sup>

<sup>a</sup> Vilnius University, Sauletekio al.9-3, LT-10222 Vilnius, Lithuania

<sup>b</sup> Cátedra de Química General, Instituto de Química Inorgánica, Facultad de Bioquímica, Química y Farmacia, Universidad Nacional de Tucumán, Ayacucho 471, 4000 San Miguel de Tucumán, Tucumán, Argentina

## ARTICLE INFO

### Article history:

Received 3 October 2017  
Received in revised form  
14 March 2018  
Accepted 24 March 2018  
Available online 24 March 2018

### Keywords:

1-Butyl-3-methylimidazolium nitrate  
Vibrational spectra  
Molecular structure  
Quantum-chemical descriptors  
DFT calculations

## ABSTRACT

The cation-anion interactions present in the 1-butyl-3-methylimidazolium nitrate ionic liquid [BMIm][NO<sub>3</sub>] were studied by using density functional theory (DFT) calculations and the experimental FT-Raman spectrum in liquid phase and its available FT-IR spectrum. For the three most stable conformers found in the potential energy surface and their 1-butyl-3-methylimidazolium [BMIm] cation, the atomic charges, molecular electrostatic potentials, stabilization energies, bond orders and topological properties were computed by using NBO and AIM calculations and the hybrid B3LYP level of theory with the 6-31G\* and 6-311++G\*\* basis sets. The force fields, force constants and complete vibrational assignments were also reported for those species by using their internal coordinates and the scaled quantum mechanical force field (SQMFF) approach. The dimeric species of [BMIm][NO<sub>3</sub>] were also considered because their presence could probably explain the most intense bands observed at 1344 and 1042 cm<sup>-1</sup> in both experimental FT-IR and FT-Raman spectra, respectively. The geometrical parameters suggest monodentate cation-anion coordination while the studies by charges, NBO and AIM calculations support bidentate coordinations between those two species. Additionally several quantum chemical descriptors were also calculated in order to interpret various molecular properties such as electronic structure, reactivity of those species and predict their gas phase behaviours.

© 2018 Elsevier B.V. All rights reserved.

## 1. Introduction

The structures of the ionic liquids are based on organic cations, such as the imidazolium, pyridinium, pyrrolidinium, tetraalkylammonium and phosphonium cations [1–17] which are weakly coordinated to inorganic or organic anions, being the most used anions bis(trifluoromethane sulfonyl)amide, trifluoromethanesulfonate, hexafluorophosphate, nitrate, dicyandiamide, tosylate, or n-alkyl sulfates among others [1,2]. The observable properties of these ionic liquids are related directly to the presence of intra- or inter-molecular interactions in their structures and, also to the orientations of cation and anion, as evidenced by using electrochemical studies for 1-butyl-3-methylimidazolium dicyanamide at the platinum-liquid interface by Aliaga and Baldelli [13]. For these reasons, the structural studies of

these species are of great interest to explain their behaviour in different media and, especially when these species interact with other [1,3,4,6,9,13,15]. For the same reasons, the vibrational studies of these ionic liquids are of great significance to identify interactions between cation and anion, as reported by Wang et al. [14] for 1-butyl-3-methylimidazolium hexafluorophosphate ionic liquid by using the <sup>31</sup>P NMR and FT-IR spectra. So far, the structural and vibrational studies of 1-butyl-3-methylimidazolium nitrate were not reported and, only the infrared spectrum and some bands were identified by Gruzdev et al. [17] while their conductivity, density and viscosity were recently reported by Bennett et al. [3]. The preparation of 1-butyl-3-methylimidazolium salts and their intra-molecular interactions were also studied by Gruzdev et al. [17] while the water effect on physicochemical properties of 1-butyl-3-methylimidazolium were published by Grishina et al. [18]. In this context, the aims of this work are: (i) to know the different types of interactions that present 1-butyl-3-methylimidazolium nitrate, such as ionic interactions (cation-anion) or of hydrogen bonds because for this ionic liquid so far

\* Corresponding author.

E-mail addresses: [sbrandan@fbqf.unt.edu.ar](mailto:sbrandan@fbqf.unt.edu.ar), [brandansa@yahoo.com.ar](mailto:brandansa@yahoo.com.ar) (S.A. Brandán).

they are not reported NBO and AIM studies [19–21], (ii) to know the structural properties of this ionic liquid because the atomic charges, bond orders, molecular electrostatic potentials, stabilization energies, topological properties were not studied for this ionic liquid and, (iii) to perform the complete vibrational assignments in order to identify this ionic liquid by using the vibrational spectroscopy and to report their force fields and force constants. Here, the theoretical calculations, based on the density functional theory (DFT) by using the hybrid B3LYP method with the 6-31G\* and 6-311++G\*\* basis sets are also useful to predict the infrared and Raman spectra which were later compared with the corresponding experimental ones in order to perform the complete assignments. The properties for the 1-butyl-3-methylimidazolium cation were also predicted in order to compare them with those obtained for their ionic liquid. The complete vibrational assignments of ionic liquid and their cation were performed taking into account their internal coordinates and corresponding force fields calculated at the same levels of theory by using the SQMFF methodology and the Molvib program [22,23] and, by using the experimental available infrared spectrum [17]. Here, the experimental Raman spectrum for [BMIm][NO<sub>3</sub>] in the liquid state was recorded by us. A 1-butyl-3-methylimidazolium nitrate dimeric species was also considered in order to explain the strong intensities of some bands observed in the vibrational spectra. This work was completed with the calculations of frontier orbitals [24,25] and quantum chemical descriptors for the ionic liquid and their cation [26–28]. After that, all properties were totally evaluated and compared for the cation and their ionic liquid.

## 2. Experimental section

FT-Raman spectra of 1-butyl-3-methylimidazolium nitrate [BMIm][NO<sub>3</sub>] were typically measured at room temperature (298 K) using the Bruker MultiRAM FT-Raman spectrometer with the motorized xyz-sample stage and with the high-sensitivity liquid nitrogen cooled germanium detector. The 1064 nm wavelength beam of the pulsed Nd:YAG laser (500 mW) as the excitation source using the 180° scattering geometry was employed in the experiments, while the resolution of the spectrometer was set to the 2 cm<sup>-1</sup>. The FT-Raman spectrum was recorded with 400 scans between 4000 and 70 cm<sup>-1</sup>. To avoid the background, samples were prepared and measured in Silica cells.

## 3. Computational details

The *GaussView* program [29] was used to model the initial structures of [BMIm][NO<sub>3</sub>] and their [BMIm] cation while the hybrid B3LYP method with the 6-31G\* and 6-311++G\*\* basis sets were employed together with the Gaussian 09 program Revision A.02 [30] to optimize both structures. It is necessary to explain that the position of the NO<sub>3</sub><sup>-</sup> anion confined in the initial structure of [BMIm][NO<sub>3</sub>] was taken in accordance to those reported in the literature for other ionic liquids [15,16,31]. The potential energy surfaces (PES) for [BMIm][NO<sub>3</sub>] by using both levels of theory were studied for variations of the dihedral N2–C12–C15–C18, C12–C15–C18–C21 and C1–H25–O26–N27 angles. Hence, four structures, named C1, C2, C3 and C4, with energies minima were found on the PES where C2 presents a global minimum by using the B3LYP/6-31G\* level of theory while C1 and C3 also present global minima by using the 6-311++G\*\* basis set, as it is observed in Table S1 and Figure S1. On the other hand, from Table S1 we clearly observed that C2 presents practically the same energy than C4 with the greater basis set and, for this reason, their properties are basically the same and, hence, the properties for C4 were not considered in this work. Fig. 1 shows the most stable structures C1, C2, C3 and C4 of [BMIm][NO<sub>3</sub>] while in Fig. 2 is presented the electronic

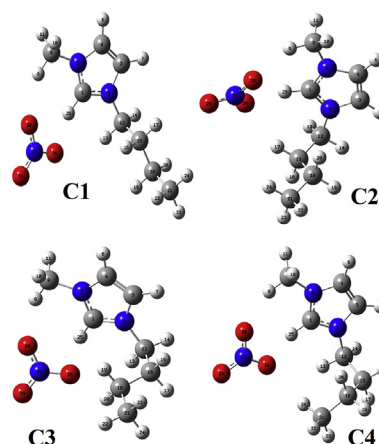


Fig. 1. The B3LYP/6-311++G\*\* optimized molecular structures of all conformers of 1-butyl-3-methylimidazolium nitrate ionic liquid with the atoms numbering.

structure of [BMIm] cation in accordance to that reported for imidazolium cation by Bennett et al. [3]. The atomic natural populations (NPA) and the Mulliken charges were studied for those three structures including the cation while the Merz-Kollman (MK) charges were employed to calculate the corresponding molecular electrostatic potentials (MEP) [32]. The topological properties were calculated employing the AIM2000 program [20] while the, bond orders expressed by Wiberg's indexes and the acceptor-donor interactions energies were obtained from NBO calculations [19]. SQMFF methodology [22] and the Molvib program [23] were used together with the corresponding normal internal coordinates in order to obtain the harmonic force fields for all species. The vibrational assignments were performed from the force fields by using the Potential Energy Distribution (PED) contributions  $\geq 10\%$  and the experimental available FT-IR spectrum of [BMIm][NO<sub>3</sub>] [17] and their experimental FT-Raman spectrum collected for only one sample -1-butyl-3-methylimidazolium nitrate by us. At this point, the dimeric structure of [BMIm][NO<sub>3</sub>] with the two nitrate anions linked to the C–H bonds belong to the rings [31] was also considered, as shown in Fig. 3. The assignments for the dimeric species were performed with the aid of the *GaussView* program [29]. Now, the predicted infrared and Raman spectra for the dimeric structure are similar to the experimental ones. Here, it is very important to mention that the calculated geometrical parameters and wavenumbers by using both basis sets were compared with the corresponding experimental values by using the root-mean-square

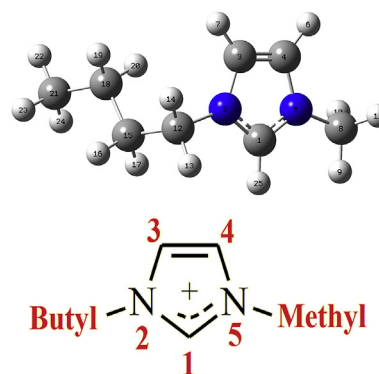
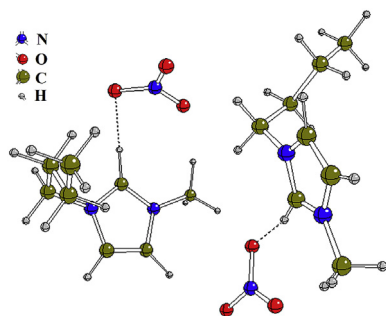


Fig. 2. Molecular theoretical structure of 1-butyl-3-methylimidazolium cation and the atoms numbering by using the B3LYP/6-311++G\*\* method (upper). A scheme of their electronic structure is also presented (bottom).



**Fig. 3.** The geometrical structure of dimer 1-butyl-3-methylimidazolium nitrate ionic liquid calculated by using B3LYP/6-311++G\*\* level. Intramolecular H-bonds are represented with dashed lines.

deviation (RMSD) values in order to find the best results and method in order to perform the corresponding assignments. For all species the volumes in gas phase were computed by using the Moldraw program [33]. The gap values for all species were calculated with the frontier orbitals [24,25] while their reactivities and behaviours were predicted by using global descriptors, as reported in the literature [26–28].

## 4. Results and discussion

### 4.1. Structural study in gas phase

In Table 1 the calculated total and relative energies are summarized, together with dipole moments, volume values and populations for the four most stable conformers of [BMIm][NO<sub>3</sub>] and, for both cation and dimer. The results by using the B3LYP/6-31G\* method show that C2 is the most stable conformer of [BMIm][NO<sub>3</sub>] with higher population while C1 and C3 are the most stable species when the 6-311++G\*\* basis set is used. Besides, C1 presents higher relative energy and dipole moment but low population in gas phase by using the B3LYP/6-31G\* method. However, when the other basis set is used, their dipole moment and population increases from 12.64 to 13.94 D and from 10.26 to 29%, respectively.

**Table 1**

Calculated total (*E*) and relative energies ( $\Delta E$ ), dipolar moment ( $\mu$ ), volume (*V*) and population values for the most stable conformers of 1-butyl-3-methyl imidazolium nitrate and their cation in gas phase.

Conformers	<i>E</i> (Hartrees)	$\Delta E$ (kJ/mol)	$\mu$ (Debye)	<i>V</i> (Å <sup>3</sup> )	Population%
B3LYP/6-31G*method/Gas phase					
1-butyl-3-methyl imidazolium nitrate					
C1	–703.6701	4.20	12.64	222.6	10.23
C2	–703.6717	0.00	11.86	221.1	56.82
C3	–703.6707	2.62	11.67	219.0	19.88
C4	–703.6703	3.67	12.04	223.1	13.07
1-butyl-3-methyl imidazolium species					
Cation	–423.1781		5.04	188.2	
Dimer	–1407.3829		6.31	454.9	
B3LYP/6-311++G**method/Gas phase					
C1	–703.8838	0.00	13.94	228.3	29
C2	–703.8835	0.79	13.51	226.7	21
C3	–703.8838	0.00	13.84	224.3	29
C4	–703.8835	0.79	13.89	226.5	21
1-butyl-3-methyl imidazolium cation					
Cation	–423.2869		4.91	191.3	
Dimer	–1407.8013		5.68	458.1	

On the other hand, the pairs of conformers C1 and C3 and, C2 and C4 have the same populations and total and relative energies by using the 6-311++G\*\* basis set. The orientations and directions of the dipole moments vectors corresponding to the four conformers change strongly in relation to the cation, as observed in Fig. 4. Obviously, the presence of two nitrate anions in the dimer evidently modifies the cation structure and, for this reason, also their properties. Hence, when two units of [BMIm][NO<sub>3</sub>] are considered by using the 6-31G\* basis set the dipole moment value decreases in the dimer to 6.31 D while its volume increases at 454.9 Å<sup>3</sup>.

The calculated geometrical parameters for [BMIm][NO<sub>3</sub>] by using the 6-31G\* level of theory compared with those obtained to the [BMIm] cation by using the RMSD values can be seen in Table 2 while in Table S2 the values for the other basis set are presented. In general, the RMSD values for C1 with the 6-31G\* basis set are different from those calculated for C2 and C3 where, obviously the better correlations are observed for C2 and C3 but, when the greater basis set is used, C3 clearly presents better correlations for bond lengths and angles (0.008 Å and 1.3°). Carefully evaluating the results, we observed that the N2–C3, C3–C4, C4–N5 and N5–C1 bond lengths practically do not change for one of the two NO<sub>3</sub><sup>–</sup> anions of the dimer. However, the values of some parameters for the second nitrate group significantly change, particularly the dihedral angles, as observed in Table 2 and S2. Besides with both basis sets, it is observed that in both monomeric and dimeric species the C1–N2 and N5–C1 bond lengths present practically double bonds characters having in the cation the same values while slightly change in the conformers of ionic liquid. On the other hand, the differences observed in the N2–C12 and N5–C8 bond lengths for the ionic liquid and their cation probably indicate that these two distances are strongly dependent on the length of side chain, thus, when the N atom is linked to the methyl group the value for N5–C8 of C2 is lower by using the 6-31G\* basis set (1.467 Å) than N2–C12 whose N atoms are linked to the butyl group (1480 Å), as observed in Table 2 and S2. When the C1–H25 distances are analyzed for all species, we observed that the cation value is lower than those corresponding to the three conformers of [BMIm][NO<sub>3</sub>], as it was expected, because the incorporation of the nitrate group to the cation generates H bond interaction between the H25 and O26 atoms and, as a consequence the enlargement of the C1–H25 bonds

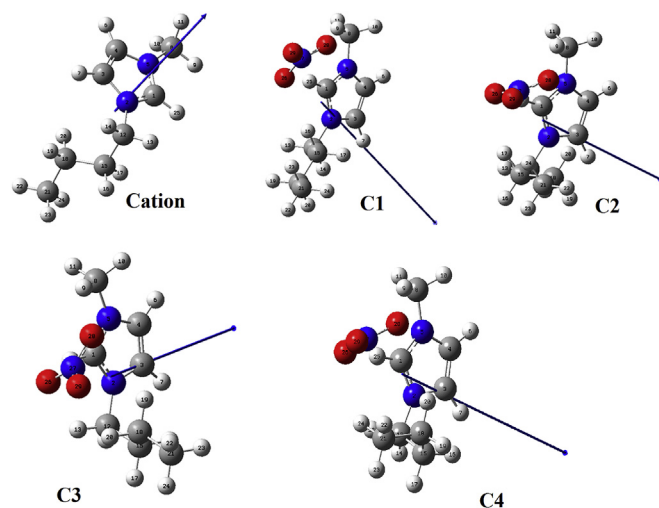


**Fig. 4.** Magnitudes and orientations of dipole moment vectors corresponding to the most stable conformers of 1-butyl-3-methylimidazolium nitrate and their cation in gas phase at the B3LYP/6-311++G\*\* level of theory.

**Table 2**  
Calculated geometrical parameters for 1-buthyl-3-methyl imidazolium nitrate monomer and dimer compared with those corresponding to the cation.

B3LYP/6-31G* Method <sup>a</sup>					
Parameters	Cation	1-buthyl-3-methyl imidazolium nitrate			
		Monomer			Dimer
		C1	C2	C3	C2
<b>Bond lengths (Å)</b>					
C1–N2	1.338	1.342	1.340	1.339	1.342/1.338
N2–C3	1.382	1.384	1.385	1.386	1.386/1.382
C3–C4	1.363	1.362	1.362	1.362	1.363
C4–N5	1.382	1.384	1.383	1.384	1.382/1.383
N5–C1	1.339	1.339	1.338	1.338	1.338/1.341
N2–C12	1.484	1.478	1.480	1.476	1.480/1.484
N5–C8	1.469	1.467	1.467	1.466	1.470/1.466
C1–H25	1.079	1.112	1.107	1.106	1.090/1.098
H25–O26		1.744	1.758	1.751	1.977/1.872
N27–O26		1.287	1.283	1.283	1.267/1.280
N27–O28		1.268	1.269	1.269	1.266/1.254
N27–O29		1.233	1.237	1.236	1.252/1.249
<b>RMSD</b>		<b>0.012</b>	<b>0.010</b>	<b>0.010</b>	
<b>Bond angles (°)</b>					
C1–N2–C3	108.2	109.0	108.9	108.9	108.4/108.7
N2–C3–C4	107.3	106.9	107.0	106.8	107.5/107.1
C3–C4–N5	107.0	106.8	106.8	106.9	106.3/106.9
C4–N5–C1	108.3	109.2	109.1	109.0	109.4/108.7
N5–C1–N2	109.0	107.8	108.0	108.1	108.1/108.4
N5–C1–H25	125.4	126.9	125.2	127.2	126.3/126.5
N2–C1–H25	125.5	125.1	126.6	124.4	125.1/124.9
C4–N5–C8	125.7	126.7	127.3	127.5	125.1/126.7
C1–N5–C8	125.9	123.9	123.3	123.3	125.3/124.5
C1–H25–O26		168.6	167.2	158.3	146.1/162.6
<b>RMSD</b>		<b>1.1</b>	<b>1.2</b>	<b>1.4</b>	
<b>Dihedral angles (°)</b>					
H25–C1–N2–C12	–2.3	1.2	2.1	–0.7	3.7/–3.4
H25–C1–N5–C8	–0.3	–1.3	0.5	–0.6	–6.3/2.7
C1–N2–C3–C4	–0.1	–0.2	–0.1	–0.3	–0.0/0.2
C3–C4–N5–C1	–0.0	–0.0	–0.1	–0.2	0.4/0.0
C12–N2–C3–C4	–178.1	–179.5	–179.1	–175.3	–177.5/–179.4
C8–N5–C4–C3	–179.3	179.4	176.2	176.3	–179.7/–179.5
<b>RMSD</b>		<b>146.4</b>	<b>145.1</b>	<b>145.2</b>	

<sup>#</sup>Values corresponding to the second nitrate group.

<sup>a</sup> This work.

is observed in the three conformers. In relation to the nitrate groups, we observed that the coordination modes of these groups with the cation is clearly monodentate because the N27–O28 and N27–O29 bond lengths have lower and different values than the N27–O26 bonds by using both basis sets. Hence, partial double bonds characters are observed in those first two bonds, especially by using the 6-311++G\*\* basis set, while the N27–O26 bonds lengths present simple bond characters because these bonds are coordinated to the cations by means of the C1–H25 bonds. Analyzing the bond angles, it is observed that for the cation all the angles by using both basis sets are practically different from those observed in the three conformers of [BMIm][NO<sub>3</sub>]. Hence, the three conformers practically show better RMSD values by using the 6-311++G\*\* basis set. Higher differences are observed in the dihedral angles showing better correlations when the 6-311++G\*\* basis set is employed. Such differences can be easily attributed to the different signs and values that present the H25–C1–N2–C12 and C8–N5–C4–C3 dihedral angles. Hence, the length of the side chain has clearly notable influence on the geometrical parameters and, especially on the dihedral angles. Hence, these values also change in the other nitrate group of dimer. Finally, the best approximation to the experimental values was obtained by using the 6-311++G\*\* basis set.

#### 4.2. Charges, molecular electrostatic potentials and bond orders studies

In this section, we have studied the atomic charges, molecular electrostatic potentials and the bond order values for [BMIm][NO<sub>3</sub>] and their cation these properties are important due to their ionic nature and to the different interactions expected for these species. Thus, the atomic Merz-Kollman (MK) and Mulliken charges were investigated for all species as a consequence of the nitrate ions present in the ionic liquid. Thus, in Table 3 the calculated MK and Mulliken charges are presented for the most stable conformers of 1-buthyl-3-methyl imidazolium nitrate together with the corresponding to the cation by using the B3LYP/6-31G\* level of theory. Table S3 shows those calculated charges by using the 6-311++G\*\* basis set. Note that the MK charges values for the four species by using both basis sets are completely different from the Mulliken ones including for a same atom the values and signs are completely different. For instance, the MK charges on the N2 atoms of the four species by using the 6-31G\* basis set have positive signs although the Mulliken ones in these species show negative signs but, by using the 6-311++G\*\* basis set all charges on the N2 atoms have positive signs in all species. On the other side, contrary results can be observed on the C3 and

**Table 3**

Calculated MK and Mulliken charges for the most stable conformers of 1-buthyl-3-methyl imidazolium nitrate compared with the corresponding to the cation.

B3LYP/6-31G* Method <sup>a</sup>									
MK					Mulliken				
Atoms	Cation	Atoms	C1	C2	C3	Cation	C1	C2	C3
1 C	-0.067	1 C	-0.137	0.000	-0.058	0.302	0.283	0.297	0.292
2 N	0.108	2 N	0.242	0.140	0.083	-0.381	-0.417	-0.413	-0.404
3 C	-0.133	3 C	-0.256	-0.292	-0.198	0.034	0.017	0.018	0.016
4 C	-0.164	4 C	-0.196	-0.165	-0.238	0.031	0.018	0.019	0.020
5 N	0.191	5 N	0.226	0.185	0.271	-0.390	-0.403	-0.400	-0.398
6 H	0.227	6 H	0.202	0.200	0.210	0.234	0.191	0.192	0.191
7 H	0.209	7 H	0.224	0.235	0.219	0.235	0.192	0.192	0.192
8 C	-0.374	8 C	-0.318	-0.359	-0.380	-0.346	-0.359	-0.349	-0.348
9 H	0.175	9 H	0.200	0.202	0.213	0.214	0.271	0.260	0.259
10 H	0.184	10 H	0.140	0.154	0.158	0.230	0.182	0.179	0.182
11 H	0.181	11 H	0.115	0.130	0.126	0.230	0.182	0.186	0.185
12 C	-0.233	12 C	-0.317	-0.147	-0.140	-0.195	-0.155	-0.160	-0.182
13 H	0.136	13 H	0.134	0.095	0.128	0.201	0.192	0.185	0.214
14 H	0.145	14 H	0.103	0.082	0.093	0.205	0.161	0.163	0.166
15 C	0.046	15 C	0.231	0.107	-0.044	-0.263	-0.291	-0.301	-0.262
16 H	0.050	16 H	0.001	0.016	0.018	0.186	0.217	0.147	0.133
17 H	0.020	17 H	-0.023	0.000	0.037	0.156	0.143	0.209	0.152
18 C	0.154	18 C	0.052	0.022	0.266	-0.271	-0.257	-0.260	-0.274
19 H	-0.002	19 H	0.010	-0.004	-0.001	0.150	0.145	0.115	0.157
20 H	-0.019	20 H	-0.009	0.041	-0.015	0.137	0.126	0.161	0.186
21 C	-0.368	21 C	-0.279	-0.302	-0.450	-0.447	-0.447	-0.457	-0.447
22 H	0.115	22 H	0.079	0.085	0.129	0.173	0.146	0.143	0.173
23 H	0.101	23 H	0.084	0.069	0.087	0.166	0.175	0.130	0.130
24 H	0.097	24 H	0.064	0.098	0.101	0.158	0.144	0.200	0.138
25 H	0.220	25 H	0.240	0.183	0.184	0.250	0.322	0.307	0.309
		26 O	-0.576	-0.553	-0.566		-0.520	-0.506	-0.516
		27 N	0.827	0.820	0.848		0.705	0.688	0.693
		28 O	-0.588	-0.566	-0.590		-0.521	-0.507	-0.513
		29 O	-0.473	-0.476	-0.492		-0.442	-0.438	-0.445

C4 atoms with both basis sets. Very important results are obtained regarding the total sum of the MK and Mulliken charges on the C1, N2 and N5 atoms that belong to the imidazole ring, in accordance to the scheme proposed in Fig. 2. We observed that the total sum of the MK charges on those three atoms result in positive values by using both basis sets while the total sum of the Mulliken charges generate negative values for the three conformers of [BMIm][NO<sub>3</sub>] with both basis sets, including the cation. Hence, the scheme presented in Fig. 2 where the ring has positive charge is better represented with the MK charges, as compared with the Mulliken ones. The Mulliken charges on the O26 and O28 atoms belong to the nitrate groups and predicted practically the same values by using 6-31G\* basis set but slightly different from those observed on the O29 atoms. Hence, this level of theory suggests bidentate coordinations of the nitrate groups in the three conformers. However, a different result is observed from the MK charges, because these charges on the O26 and O28 atoms are unlike between the three O atoms.

In Table 4 the molecular electrostatic potentials (MEP) are summarized for the three conformers of [BMIm][NO<sub>3</sub>] and their cation by using the B3LYP/6-31G\* level of theory while these values by using the other basis set is presented in Table S4. The mapped surfaces for all species are represented graphically in Fig. 5. The results of Table 4 shows clearly that the MEPs values on all atoms slightly change from cation to the three conformers but the most significant changes are observed on the C1, N2 and N5 atoms located in the rings, in accordance with the corresponding MK charges. Besides, the H25 atoms belong to the C1–H25 bonds also change significantly due to the H bonds formed as a consequence of the coordination of those atoms with the nitrate groups. Here, another very important result is observed in the similar MEP values on the O26, O28 and O29 atoms by using both basis sets indicating probable monodentate coordination for the nitrate groups. If now,

we analyzed the different colorations observed from Fig. 5, we observed that the expected blue color that is observed on the cation

**Table 4**

Calculated molecular electrostatic potentials for 1-buthyl-3-methyl imidazolium nitrate compared with the corresponding to the cation.

B3LYP/6-31G* Method <sup>a</sup>					
Atoms	Cation	Atoms	C1	C2	C3
1 C	-14.474	1 C	-14.642	-14.640	-14.641
2 N	-18.090	2 N	-18.231	-18.232	-18.233
3 C	-14.523	3 C	-14.652	-14.654	-14.655
4 C	-14.523	4 C	-14.654	-14.655	-14.654
5 N	-18.083	5 N	-18.229	-18.231	-18.231
6 H	-0.900	6 H	-1.025	-1.026	-1.026
7 H	-0.902	7 H	-1.024	-1.026	-1.026
8 C	-14.528	8 C	-14.676	-14.674	-14.672
9 H	-0.928	9 H	-1.082	-1.081	-1.078
10 H	-0.934	10 H	-1.073	-1.070	-1.069
11 H	-0.935	11 H	-1.075	-1.074	-1.073
12 C	-14.533	12 C	-14.659	-14.659	-14.663
13 H	-0.946	13 H	-1.076	-1.076	-1.077
14 H	-0.947	14 H	-1.068	-1.070	-1.074
15 C	-14.599	15 C	-14.726	-14.729	-14.719
16 H	-0.986	16 H	-1.117	-1.111	-1.106
17 H	-0.987	17 H	-1.111	-1.120	-1.106
18 C	-14.616	18 C	-14.728	-14.740	-14.747
19 H	-1.009	19 H	-1.122	-1.131	-1.139
20 H	-1.008	20 H	-1.121	-1.135	-1.142
21 C	-14.645	21 C	-14.747	-14.765	-14.756
22 H	-1.027	22 H	-1.127	-1.143	-1.139
23 H	-1.027	23 H	-1.130	-1.143	-1.135
24 H	-1.026	24 H	-1.127	-1.149	-1.136
25 H	-0.870	25 H	-1.039	-1.039	-1.040
		26 O	-22.377	-22.371	-22.374
		27 N	-18.148	-18.143	-18.146
		28 O	-22.379	-22.372	-22.375
		29 O	-22.380	-22.374	-22.377

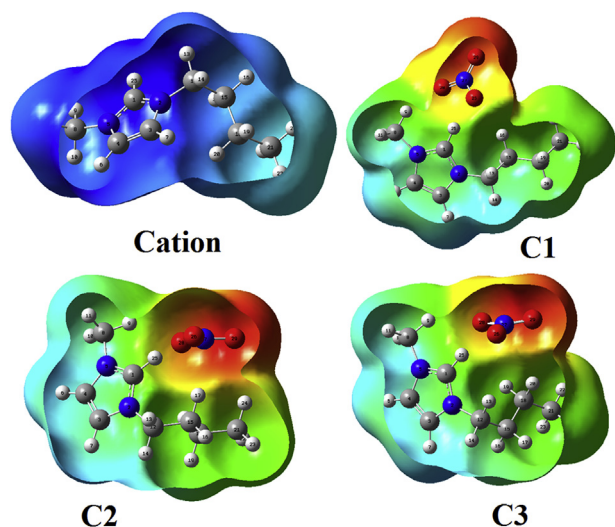


**Fig. 5.** Molecular electrical potential surfaces of 1-butyl-3-methylimidazolium nitrate and their cation obtained from B3LYP/6-311++G\*\*. Color ranges, in au: from red  $-0.090$  to blue  $+0.090$  and isodensity value of  $0.005$ . (For interpretation of the references to colour in this figure legend, the reader is referred to the Web version of this article.)

clearly represents electrophilic sites while the red and green colours indicate nucleophilic and inert sites, respectively. Here, the red colours observed on the nitrate groups of the three conformers indicate nucleophilic places due to the anionic characteristics of those groups while on the C–H bonds of the rings and, on part of the C–H belong to the CH<sub>3</sub> groups blue colours are observed because these sites are electrophilic places. Finally, on the butyl side chain green colours are observed indicating clearly that these sites are completely inert.

In relation to the bond orders, in Table 5, the bond orders (BO) expressed by Wiberg's indexes for 1-butyl-3-methyl imidazolium nitrate are given in Table 5 together with the cation while in Table S5 these values are presented by using the other basis set. The bond order values were calculated with the NBO program [19] because they are very useful to indicate the characteristics of the different bonds. In general, the addition of nitrate group to the cation clearly increases the BO of some atoms, as observed by using the 6-31G\* basis set. However, when the other basis set is used few atoms decrease their values, as can be seen in Table S5. The BO values for the O26 and O28 atoms belonging to the nitrate groups in the three conformers have approximately the same and low BO values (O–N–O) than those corresponding to the O29 atoms (N=O) which present higher values by using the 6-31G\* basis set. But when the other basis set is employed the three O atoms present approximately the same BO values. Evidently, here different coordination modes by using both basis set are predicted for the nitrate groups.

#### 4.3. Energy interactions and topological studies

The above studies by using MK and Mulliken charges, MEPs and bond orders have suggested different coordination modes of the nitrate groups in the three conformers of [BMIm][NO<sub>3</sub>] and, for these reasons, the donor-acceptor energy interactions and the topological properties for all species are necessary in order to elucidate the type of interactions that is present in these species. Hence, NBO [19] and AIM calculations were performed to analyze the stabilities of these species by using the topological properties calculated with the AIM2000 program [20] and the Bader's theory

**Table 5**

Calculated bond orders expressed, as Wiberg indexes by atoms, for the three conformers of 1-butyl-3-methyl imidazolium nitrate compared with the corresponding to the cation.

B3LYP/6-31G* Method <sup>a</sup>					
Atoms	Cation	Atoms	C1	C2	C3
1 C	2.747	1 C	3.730	3.742	3.738
2 N	2.649	2 N	3.514	3.513	3.514
3 C	2.897	3 C	3.876	3.875	3.876
4 C	2.883	4 C	3.877	3.876	3.877
5 N	2.669	5 N	3.523	3.523	3.517
6 H	0.800	6 H	0.935	0.935	0.935
7 H	0.802	7 H	0.935	0.935	0.935
8 C	2.990	8 C	3.710	3.715	3.718
9 H	0.751	9 H	0.915	0.918	0.917
10 H	0.734	10 H	0.943	0.943	0.943
11 H	0.734	11 H	0.945	0.944	0.944
12 C	3.078	12 C	3.811	3.811	3.801
13 H	0.739	13 H	0.937	0.937	0.929
14 H	0.740	14 H	0.945	0.945	0.942
15 C	3.110	15 C	3.880	3.879	3.902
16 H	0.745	16 H	0.928	0.942	0.951
17 H	0.742	17 H	0.948	0.931	0.942
18 C	3.145	18 C	3.905	3.904	3.889
19 H	0.735	19 H	0.948	0.956	0.947
20 H	0.738	20 H	0.953	0.946	0.938
21 C	3.060	21 C	3.843	3.837	3.848
22 H	0.749	22 H	0.946	0.947	0.939
23 H	0.745	23 H	0.943	0.955	0.955
24 H	0.744	24 H	0.951	0.937	0.953
25 H	0.797	25 H	0.917	0.918	0.917
		26 O	1.852	1.863	1.860
		27 N	4.076	4.077	4.077
		28 O	1.858	1.866	1.861
		29 O	1.989	1.977	1.975

[21]. These donor-acceptor energy interactions for the three conformers of 1-butyl-3-methyl imidazolium nitrate compared with the corresponding to the cation can be seen in Table 6 while in Table S6 their values are observed with the other basis set. These energy interactions are calculated from the NBO program by using the Second Order Perturbation Theory Analysis of Fock Matrix in NBO Basis, which are expressed as  $E(2)$ . The deep analysis of these results clearly shows the differences that present the three conformers of [BMIm][NO<sub>3</sub>] and their cation. Obviously, the cation is a charged species and, for this reason, it is an unstable species with low donor-acceptor energy interactions, as compared with the neutral species. A total of six interactions are observed for the three conformers but in the cation the  $\Delta ET_{LP \rightarrow \sigma^*}$  and  $\Delta ET_{\pi \rightarrow \sigma^*}$  interactions related to the nitrate groups are not observed, as it is expected. Here, the total energy donor-acceptor energy interactions values for C1 and C2 conformers by using both basis sets are higher than those corresponding to C3, being the most stable the C1 conformer by using the 6-31G\* basis set but C2 is the most stable species by using the other one. Here, higher stabilities of C1 and C2 are clearly attributed to the  $\pi C1-N2 \rightarrow LPN5$  and  $\pi C3-C4 \rightarrow LPN5$  interactions which are not present in C3. Probably, these results could in part be justified by the higher dipole moment values which are observed for both C1 and C2 species and by the higher values of the C1–H25–O26 bond angles observed from Table 2 for those two species ( $168.6^\circ$  in C1,  $167.2^\circ$  in C2 and  $158.3^\circ$  in C3). When the greatest basis set is used a new  $\Delta ET_{\sigma \rightarrow \sigma^*}$  interaction appears which can only be observed in C3. Thus, the total energies support high stabilities for the three species but specifically for C1 by using the 6-31G\* basis set and for C2 by using the greatest basis set.

The atom in molecules (AIM) Bader's theory is useful to analyze the intra-molecular and inter-molecular interactions that present different species by using their topological properties [21]. Hence,

**Table 6**

Main donor-acceptor energy interactions (in kJ/mol) for the three conformers of 1-butyl-3-methyl imidazolium nitrate compared with the corresponding to the cation.

B3LYP/6-31G*				
Delocalization	Cation	C1	C2	C3
$\pi$ C1–N2 $\rightarrow$ LPN5	95.60	90.33	89.37	
$\pi$ C3–C4 $\rightarrow$ LPN5	0.00	549.00	547.75	
$\Delta E_{T\pi \rightarrow LP}$	<b>95.60</b>	<b>639.33</b>	<b>637.12</b>	
$\pi$ C1–N2 $\rightarrow$ $\pi^*$ C3–C4	71.48	77.96	76.91	76.49
$\pi$ C3–C4 $\rightarrow$ $\pi^*$ C1–N2	62.41	49.07	48.91	48.24
$\Delta E_{T\pi \rightarrow \pi^*}$	<b>133.89</b>	<b>127.03</b>	<b>125.82</b>	<b>124.73</b>
LPN5 $\rightarrow$ $\pi^*$ C1–N2	332.10	326.63	328.76	326.33
LPN5 $\rightarrow$ $\pi^*$ C3–C4	125.07	136.98	137.40	136.90
LPO26 $\rightarrow$ $\pi^*$ N27–O29		404.42	304.76	276.97
LPO28 $\rightarrow$ $\pi^*$ N27–O29		484.09	339.79	306.02
$\Delta E_{TLP \rightarrow \pi^*}$	<b>457.17</b>	<b>1352.10</b>	<b>1110.71</b>	<b>1046.21</b>
LPO26 $\rightarrow$ $\sigma^*$ C1–H25		111.48	87.82	87.11
LPO26 $\rightarrow$ $\sigma^*$ N27–O29		61.78	67.59	67.17
LPO28 $\rightarrow$ $\sigma^*$ O26–N27		53.17	53.92	54.38
LPO28 $\rightarrow$ $\sigma^*$ N27–O29		69.56	68.84	67.84
LPO29 $\rightarrow$ $\sigma^*$ O26–N27		83.47	80.76	80.47
LPO29 $\rightarrow$ $\sigma^*$ N27–O28		79.55	78.79	79.50
$\Delta E_{TLP \rightarrow \sigma^*}$		<b>459.01</b>	<b>437.73</b>	<b>436.48</b>
$\pi^*$ C1–N2 $\rightarrow$ $\pi^*$ C3–C4	70.98	104.04	102.91	104.67
$\pi^*$ N27–O29 $\rightarrow$ $\pi^*$ N27–O29		48.03	45.48	43.68
$\Delta E_{T\pi \rightarrow \pi^*}$	<b>70.98</b>	<b>152.07</b>	<b>148.39</b>	<b>148.35</b>
$\pi^*$ N27–O29 $\rightarrow$ $\sigma^*$ N27–O29			104.79	141.08
$\Delta E_{T\pi \rightarrow \sigma^*}$			104.79	141.08
$\Delta E_{Total}$	<b>757.63</b>	<b>2729.54</b>	<b>2564.55</b>	<b>1896.85</b>

the electron density,  $\rho(r)$  and the Laplacian values,  $\nabla^2\rho(r)$  were calculated for the three conformers of [BMIm][NO<sub>3</sub>] and their cation in the bond critical points (BCPs) by using the AIM 2000 program [20]. The results of those two properties obtained for all species can be seen in Table 7 while in Table S7 the results for the other basis set are summarized. Here, only the interactions for the three conformers were presented because there are not observed

**Table 7**

Analysis of the topological properties for the three conformers of 1-butyl-3-methyl imidazolium nitrate compared with the corresponding to the cation.

B3LYP/6-31G*					
C1					
Parameter (a.u.)	H9...O28	H16...O26	H25...O26		
$\rho(r_c)$	0.0202	0.0122	0.0459		
$\nabla^2\rho(r_c)$	0.0644	0.0380	0.1338		
Distances (Å)	2.1030	2.3820	1.7440		
C2					
Parameter (a.u.)	H9...O28	H17...O26	H25...O26	H24...O29	H20...O28
$\rho(r_c)$	0.0173	0.0121	0.0443	0.0075	0.0032
$\nabla^2\rho(r_c)$	0.0542	0.0384	0.1307	0.0260	0.0134
Distances (Å)	2.2030	2.3960	1.7580	2.5800	3.0100
C3					
Parameter (a.u.)	H9...O28		H25...O26	H20...O29	
$\rho(r_c)$	0.0152		0.0451	0.0066	
$\nabla^2\rho(r_c)$	0.0494		0.1357	0.0265	
Distances (Å)	2.2550		1.7510	2.7060	

interactions for the cation. It is necessary to clarify that in  $\nabla^2\rho(r) > 0$  and  $|\lambda_1/\lambda_3| < 1$  the interactions are of the H bonds, in accordance with the Bader's theory [21]. Here, the eigenvalues ( $\lambda_1, \lambda_2, \lambda_3$ ) of the Hessian matrix were not presented. Table 7 and S7 show H bonds formations in the three conformers; having C1 and C3 three H bonds of different characteristics while in C2 the number of H bonds increases to five. Note that by using the 6-31G\* basis set the H9...O28 and H25...O26 interactions are present in the three conformers and, that the density observed for the H25...O26 interaction is higher in the C1 conformer probably because the distance between those two atoms is lower. With the other basis set the number of interactions decreases for C1 from 3 to 2 and for C2 from 5 to 3 while for C3 the number of interactions does not change. Those two interactions clearly support the bidentate coordination for the three conformers. Clearly, C2 has the higher number of H bonds and, as a consequence, higher stability is expected for this conformer by using the 6-31G\* basis set but, when the other basis set is employed C2 presents the same stability than C3. Obviously, the basis set has notable influence on the H bonds interactions and, hence, on their stabilities.

#### 4.4. Evaluation of gap energies and global descriptors

The energy difference between the HOMO and LUMO frontier orbitals (gap) is important to predict the reactivities of diverse species, in accordance to Parr and Pearson [24] and Brédas [25]. Thus, the HOMO and LUMO orbitals, defined as highest occupied molecular orbital and the lowest unoccupied molecular orbital respectively, are also practical to calculate useful descriptors that are necessary to predict the behaviour of the species in different media [26–28]. Hence, in Table 8 the calculated frontier orbitals, energy band gap, chemical potential ( $\mu$ ), electronegativity ( $\chi$ ), global hardness ( $\eta$ ), global softness ( $S$ ), global electrophilicity index ( $\omega$ ) and global nucleophilicity index ( $E$ ) for [BMIm][NO<sub>3</sub>] and their cation are compared with the values obtained for p-xylylenediaminium bis(nitrate) and their cation [34]. Then, in Table S8 the values by using the 6-311++G\*\* basis set are presented. If first, the gap values for the three conformers and their cation are compared by using the 6-31G\* basis set, we observed the same values for C2 and the cation (–4.36 eV) and for C1 and C3 (–4.3764 eV) where the two first have lower values than the second ones, for these reasons, these two C1 and C3 species have slightly low reactivities as compared with those two species. When these gap values are compared by using the B3LYP/6-311++G\*\* method the cation and C2 are the most reactive species but the three conformers of ionic liquid are more reactive than their cation and than the p-xylylenediaminium and their cation [39]. Note that the p-xylylenediaminium cation is less reactive than the [BMIm] one by using the 6-31G\* basis set but on the contrary is observed with the other basis set. Analyzing the descriptors, we observed that despite C2 and the [BMIm] cation and C1 and C3 have the same gap values all species, they show different softness values by using both basis sets. In relation to the electrophilicity and nucleophilicity indexes, it is observed that the cations of both nitrate species present higher indexes than the corresponding neutral species but these values are higher for p-xylylenediaminium bis(nitrate) in relation to the ionic liquid probably because this species has two nitrate groups in their structure while the ionic liquid presents only one nitrate group. Both cations are positively charged species and electrophilics and, for these reasons, they have higher electrophilicity indexes. These descriptors are compared in Table 8 and S8 with other reported for species with different properties, such as, the two antimicrobial tautomers of 1,3-benzothiazole, thione and thiol [35], the antiviral thymidine [36] and with the toxic species CN<sup>–</sup>, CO and saxitoxin

**Table 8**  
Calculated HOMO and LUMO orbitals, energy band gap, chemical potential ( $\mu$ ), electronegativity ( $\chi$ ), global hardness ( $\eta$ ), global softness ( $S$ ), global electrophilicity index ( $\omega$ ) and global nucleophilicity index ( $E$ ) for [BMIm][NO<sub>3</sub>] and their cation.

B3LYP/6-31G* method <sup>a</sup>					B3LYP/6-311++G** <sup>b</sup>	
Frontier orbitals (eV)	[BMIm]	[BMIm][NO <sub>3</sub> ]		C3	p-Xylylenediaminium	p-xylylenediaminium bis(nitrate)
	Cation	C1	C2		Cation	neutral
HOMO	-11.6033	-5.0336	-5.1743	-5.0980	-14.4150	-7.5729
LUMO	-4.8613	-0.8388	-0.8143	-0.7216	-8.5800	-1.8621
GAP	-4.3600	-4.3764	-4.3600	-4.3764	-5.8350	-5.7108
Descriptors (eV)						
$\chi$	-3.3710	-2.0974	-2.1800	-2.1882	-2.9175	-2.8554
$\mu$	-8.2323	-2.9362	-2.9943	-2.9098	-11.4975	-4.7175
$\eta$	3.3710	2.0974	2.1800	2.1882	2.9175	2.8554
$S$	0.1483	0.2384	0.2294	0.2285	0.1714	0.1751
$\omega$	10.0520	2.0552	2.0564	1.9347	22.6551	3.8970
$E$	-27.7511	-6.1584	-6.5276	-6.3672	-33.5440	-13.4703
B3LYP/6-31G*						
Frontier orbitals (eV)	Thionec	Thiol <sup>c</sup>	Thymidine <sup>d</sup>	CN <sup>-e</sup>	CO <sup>e</sup>	Saxitoxin <sup>e</sup>
HOMO	-6.4443	-6.8847	-6.9621	-21.0491	-10.1077	-13.656
LUMO	-2.7918	-2.6194	-1.4443	-18.8917	-0.5926	-7.1273
GAP	-3.6525	-4.2653	-5.5178	-2.1574	-9.5151	-6.5287
Descriptors (eV)						
$\chi$	-1.8263	-2.1327	-2.7589	-1.0787	-4.7576	-3.2644
$\mu$	-4.61805	-4.7521	-4.2032	-19.9704	-5.3502	-10.3917
$\eta$	1.8263	2.1327	2.7589	1.0787	4.7576	3.2644
$S$	0.2738	0.2345	0.1812	0.4635	0.1051	0.1532
$\omega$	5.8388	5.2943	3.2018	184.8600	3.0083	16.5403
$E$	-8.4337	-10.1345	-11.5962	-21.5421	-25.4536	-33.9220

$$\chi = -[E(\text{LUMO}) - E(\text{HOMO})]/2; \mu = [E(\text{LUMO}) + E(\text{HOMO})]/2; \eta = [E(\text{LUMO}) - E(\text{HOMO})]/2.$$

$$S = 1/2\eta; \omega = \mu^2/2\eta; E = \mu^*\eta.$$

<sup>a</sup> This work.

<sup>b</sup> From Ref [34].

<sup>c</sup> From Ref [35].

<sup>d</sup> From Ref [36].

<sup>e</sup> From Ref [28].

[28]. Here, we observed that the electrophilicity index values for the three conformers of the ionic liquid by using both basis sets are closer to the values observed for CO while their cation also presents nucleophilicity index closer to toxic agent CO [28]. Note that the nucleophilicity indexes for the three conformers with the 6-311++G\*\* basis set are closer to thione [35]. With the greater basis set, C2 is the most reactive conformer including those two compared species while the compared cations have high values of electrophilicity and nucleophilicity indexes. These latter indexes calculated with the 6-311++G\*\* basis set are closer to the value observed for thione [35]. Thus, these results clearly evidence that the basis set has remarkable influence on the reactivities and behaviors of these species in gas phase.

## 5. Vibrational analysis

In this analysis, the optimized structures in gas phase of the three conformers of [BMIm][NO<sub>3</sub>] with monodentate coordination and their cation were considered by using the B3LYP/6-311++G\*\* method, in accordance to their calculated low RMSD values for both geometries and wavenumbers. Hence, all monomeric structures were optimized with C<sub>1</sub> symmetries where the monomers and their cation present 81 and 69 vibration normal modes, respectively and, where all modes present activity in both spectra. The FT-IR spectrum was taken from that reported for [BMIm][NO<sub>3</sub>] in liquid phase by Gruzdev et al. [17] while their FT-Raman

spectrum was recorded by us. Both spectra are respectively given in Figs. 6 and 7, compared with the corresponding predicted for the most stable monomers C1 and C3 and the dimer. In those two figures we observed good correlations among the experimental and the predicted spectra when the dimeric species are considered. In particular, the Raman spectra shows a very good correlation when the predicted spectrum expressed in activities are corrected to intensities by using equations reported in the literature [37,38]. The band observed in the infrared spectrum at 3490 cm<sup>-1</sup> can be assigned to the OH stretching modes of water, as reported by Gruzdev et al. [17] because during the preparation of this ionic liquid the reactives are dissolved in water. On the other hand, the band at 2386 cm<sup>-1</sup> is clearly attributed by Gruzdev et al. [17] to the cation-anion interaction between the imidazole ring and the nitrate groups. Here, the very strong band observed in the IR spectrum at 1344 cm<sup>-1</sup>, which is assigned to vibrations NO<sub>3</sub><sup>-</sup> by Gruzdev et al. [17], is predicted with low intensity in the IR spectra of the monomer while the intensity of this band is increased in the dimer. In the same way, the band at 1362 cm<sup>-1</sup> predicted in the Raman spectrum with low intensity is clearly increased in the dimer. Besides, the groups of bands located in the higher wavenumbers region in the Raman spectrum of the monomer are visibly predicted with higher intensities than in the dimer. Hence, the presence of the dimer could probably justify the strong intensities of those bands in both spectra. On the other side, the strong Raman band at 1417 cm<sup>-1</sup> could also justify the presence of the dimer because a

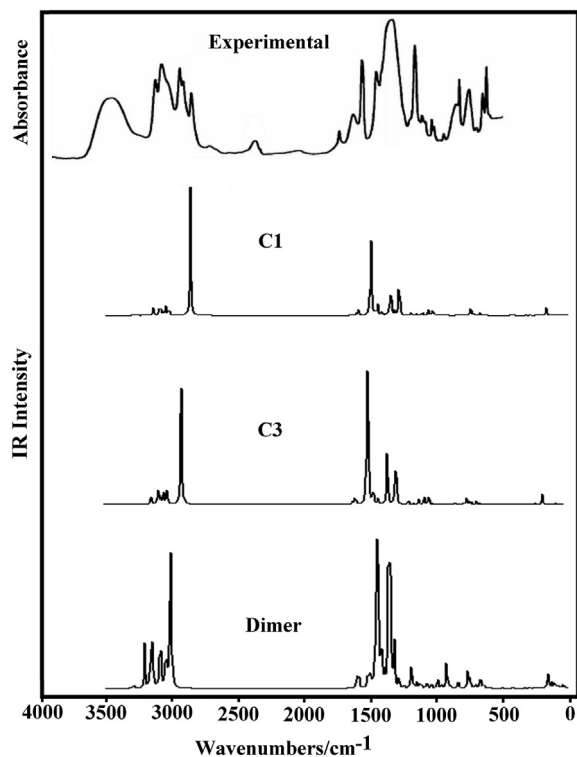


**Fig. 6.** Comparison of experimental FTIR spectrum [17] with predicted (B3LYP/6-311++G\*\*) gas phase infrared spectra for the most stable monomers C1 and C3 and the dimer of the most stable conformer of 1-butyl-3-methylimidazolium nitrate.

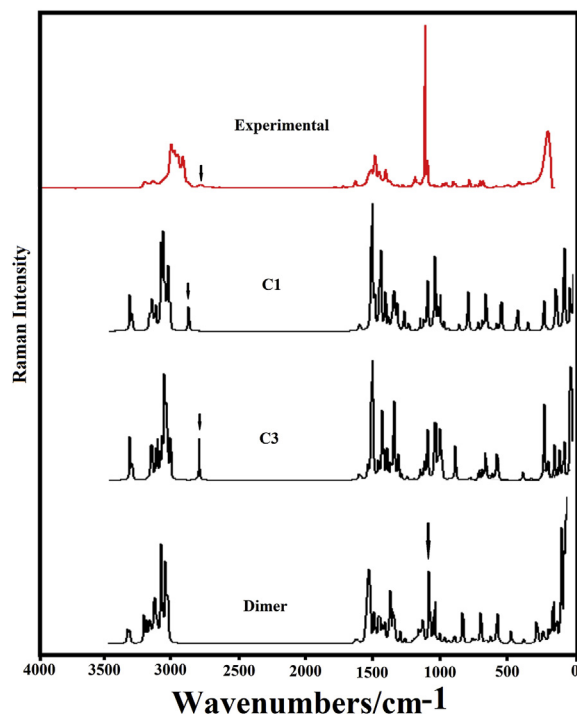


**Fig. 7.** Experimental Raman spectrum of 1-butyl-3-methylimidazolium nitrate compared with the predicted for the most stable structures of monomer and dimer in the gas phase at B3LYP/6-311++G\*\* level of theory.

symmetric  $\text{CH}_3$  deformation mode is predicted in this species at  $1416\text{ cm}^{-1}$ . Here, the differences observed between both

experimental and predicted spectra can be in part attributed to the calculations because they were performed in gas phase where the packing forces were not considered. The force fields of those monomer and cation species were computed by using the internal coordinates and the SQMFF procedure [22] with the Molvib program [23] and considering harmonic force fields. The scale factors used in the refinement process to obtain the harmonic scaled force fields were those reported in the literature [22]. In Table 9 the observed and calculated wavenumbers are presented together with assignments for the monomers and dimer of 1-butyl-3-methylimidazolium nitrate and their cation in gas phase by using the B3LYP/6-311++G\*\* level of theory. Here, the better approximations are obtained with that method because the initial RMSD values for C1, C2, C3 and their cation are respectively 46.70, 45.21, 48.20 and  $68.12\text{ cm}^{-1}$  while the final values decrease up to 19.73, 19.01, 18.03 and  $24.14\text{ cm}^{-1}$ , respectively. These values are also presented in Table 9. The complete assignments for the three monomers and their cation were performed using the potential energy distribution (PED) contributions  $\geq 10\%$  and the corresponding experimental spectra while for the dimer the assignments were performed with the GaussView program [29]. We have discussed below only the assignments performed for the most important groups of [BMIm][ $\text{NO}_3$ ] and their cation (see Table 9).

## 5.1. Bands assignments

### 5.1.1. C–H modes

For the three conformers of [BMIm][ $\text{NO}_3$ ] and their cation are expected the stretching, in-plane and out-of-plane deformation modes due to the C1–H25, C3–H7 and C4–H6 groups that belong to the imidazoline rings. Here, in the three conformers and their cation the C3–H7 and C4–H6 stretching modes are predicted coupled between them by SQM calculations in the  $3156\text{--}3139\text{ cm}^{-1}$  region while in the dimer these modes are predicted between  $3203$  and  $3007\text{ cm}^{-1}$  and, for these reasons, those modes are assigned between  $3170/3163$  and  $2942/2941\text{ cm}^{-1}$ . As expected, in the four species the symmetrical modes are assigned to the Raman band of medium intensity at  $3163\text{ cm}^{-1}$  while the corresponding antisymmetric modes can be assigned to the IR bands at  $3147$  and  $3101\text{ cm}^{-1}$ . Note that in the three conformers of [BMIm][ $\text{NO}_3$ ] the C1–H25 stretching modes are predicted at  $2793$  and  $2717\text{ cm}^{-1}$ , hence, they are easily assigned to the IR and Raman bands at  $2743$  and  $2738\text{ cm}^{-1}$ , respectively. In the cation, the C1–H25 stretching mode is predicted at  $3142\text{ cm}^{-1}$  and assigned to the IR band at  $3147\text{ cm}^{-1}$ . Obviously, the presences of the nitrate groups shift these modes toward lower wavenumbers in the three conformers. However, the C1–H25 in-plane deformation modes are predicted in all conformers between  $1312$  and  $1307\text{ cm}^{-1}$  while in the cation this mode is predicted at  $1134\text{ cm}^{-1}$ . Hence, those modes are assigned in the predicted regions by SQM calculations. The other C3–H7 and C4–H6 in-plane deformation modes are predicted in the cation to higher wavenumbers ( $1272/1095\text{ cm}^{-1}$ ) than the three conformers ( $1081$  and  $1078\text{ cm}^{-1}$ ). Thus, these modes are assigned between  $1272$  and  $1078\text{ cm}^{-1}$ . In the dimer these modes are predicted between  $1319$  and  $1191\text{ cm}^{-1}$ .

### 5.1.2. $\text{CH}_3$ modes

In the monomers and cation a total of 18 vibration normal modes are expected because there are two  $\text{CH}_3$  groups in their structures. Hence, the antisymmetric modes were predicted between  $3033$  and  $2959\text{ cm}^{-1}$  while the symmetric modes between  $2942$  and  $2893\text{ cm}^{-1}$ . Hence, the Raman bands of the medium intensities at  $2941$ ,  $2913$  and  $2874\text{ cm}^{-1}$  are assigned to those symmetrical modes. The deformation modes are predicted in species containing these groups between  $1474$  and  $1366\text{ cm}^{-1}$  [26,36,39],

Table 9

Observed and calculated wavenumbers ( $\text{cm}^{-1}$ ) and assignments for the most stable conformers of 1-buthyl-3-methyl imidazolium nitrate and their cation and dimer in gas phase.

Experimental		Monomer								Dimer <sup>a</sup>	
IR <sup>b</sup>	Ra <sup>a</sup>	Cation <sup>a</sup>		C1 <sup>a</sup>		C2 <sup>a</sup>		C3 <sup>a</sup>		Calc <sup>d</sup>	Assignment <sup>a</sup>
		SQM <sup>c</sup>	Assignment <sup>a</sup>	SQM <sup>c</sup>	Assignment <sup>a</sup>	SQM <sup>c</sup>	Assignment <sup>a</sup>	SQM <sup>c</sup>	Assignment <sup>a</sup>		
3170sh	3163 m									3203	vC–H
3170sh	3163 m	3156	v <sub>s</sub> C–H	3155	v <sub>s</sub> C–H	3156	v <sub>s</sub> C–H	3154	v <sub>s</sub> C–H	3163	v <sub>a</sub> CH <sub>3</sub>
3147 m	3147sh	3142	vC1–H25	3137	v <sub>a</sub> C–H	3139	v <sub>a</sub> C–H	3137	v <sub>a</sub> C–H	3151	vC–H
3101s	3101w	3139	v <sub>a</sub> C–H	3011	v <sub>a</sub> CH <sub>3</sub> (C8)	3007	v <sub>a</sub> CH <sub>3</sub> (C8)	3013	v <sub>a</sub> CH <sub>3</sub> (C8)	3144	vC–H
3101s	3101w	3033	v <sub>a</sub> CH <sub>3</sub> (C8)	3000	v <sub>a</sub> CH <sub>3</sub> (C8)	2998	v <sub>a</sub> CH <sub>3</sub> (C8)	3000	v <sub>a</sub> CH <sub>3</sub> (C8)	3131	v <sub>a</sub> CH <sub>3</sub>
3057sh	3022sh	3018	v <sub>a</sub> CH <sub>3</sub> (C8)							3050	v <sub>s</sub> CH <sub>2</sub>
2988sh	2988sh	2995	v <sub>a</sub> CH <sub>2</sub> (C12)	2992	v <sub>a</sub> CH <sub>2</sub> (C12)	2977	v <sub>a</sub> CH <sub>2</sub> (C12)	2993	v <sub>a</sub> CH <sub>2</sub> (C12)	3007	vC–H
2962s	2962 m	2979	v <sub>a</sub> CH <sub>3</sub> (C21)	2967	v <sub>a</sub> CH <sub>3</sub> (C21)	2969	v <sub>a</sub> CH <sub>3</sub> (C21)	2967	v <sub>a</sub> CH <sub>3</sub> (C21)	3003	v <sub>s</sub> CH <sub>2</sub>
2962s	2962 m	2967	v <sub>a</sub> CH <sub>3</sub> (C21)	2959	v <sub>a</sub> CH <sub>3</sub> (C21)	2960	v <sub>a</sub> CH <sub>3</sub> (C21)	2955	v <sub>a</sub> CH <sub>3</sub> (C21)	2998	v <sub>s</sub> CH <sub>2</sub>
2953sh		2951	v <sub>s</sub> CH <sub>2</sub> (C12)								
2942sh	2941 m	2942	v <sub>s</sub> CH <sub>3</sub> (C8)	2942	v <sub>a</sub> CH <sub>2</sub> (C15)	2943	v <sub>a</sub> CH <sub>2</sub> (C15)	2940	v <sub>s</sub> CH <sub>2</sub> (C12)		
2942sh	2941 m	2937	v <sub>a</sub> CH <sub>2</sub> (C15)	2932	v <sub>s</sub> CH <sub>2</sub> (C12)	2929	v <sub>s</sub> CH <sub>2</sub> (C12)	2932	v <sub>a</sub> CH <sub>2</sub> (C18)		
2924sh	2913 m			2920	v <sub>s</sub> CH <sub>3</sub> (C8)	2915	v <sub>s</sub> CH <sub>3</sub> (C8)	2921	v <sub>s</sub> CH <sub>3</sub> (C8)		
2924sh	2913 m	2909	v <sub>a</sub> CH <sub>2</sub> (C18)	2917	v <sub>a</sub> CH <sub>2</sub> (C18)	2909	v <sub>a</sub> CH <sub>2</sub> (C18)	2918	v <sub>a</sub> CH <sub>2</sub> (C15)		
2924sh	2913 m	2907	v <sub>s</sub> CH <sub>3</sub> (C21)	2898	v <sub>s</sub> CH <sub>3</sub> (C21)	2900	v <sub>s</sub> CH <sub>3</sub> (C21)	2897	v <sub>s</sub> CH <sub>2</sub> (C18)		
2875s	2874 m	2898	v <sub>s</sub> CH <sub>2</sub> (C15)	2891	v <sub>s</sub> CH <sub>2</sub> (C15)	2897	v <sub>s</sub> CH <sub>2</sub> (C15)	2893	v <sub>s</sub> CH <sub>3</sub> (C21)		
2875s	2874 m	2882	v <sub>s</sub> CH <sub>2</sub> (C18)	2885	v <sub>s</sub> CH <sub>2</sub> (C18)	2872	v <sub>s</sub> CH <sub>2</sub> (C18)	2884	v <sub>s</sub> CH <sub>2</sub> (C15)		
2743w	2738w			2743	vC1–H25	2717	vC1–H25	2793	vC1–H25		
1646w	1662w									1608	vC=C, vC=N
1579s	1569w	1548	vC3–C4, vN5–C1	1550	vC3–C4	1550	vN5–C1	1550	vC3–C4	1599	vC=C, vC=N
1579s	1569w	1539	vN2–C1	1534	βC1–H25	1539	vC3–C4, vN2–C1	1533	vN2–C1	1582	vC=C, vC=N
1465s	1450 m	1449	δ <sub>a</sub> CH <sub>3</sub> (C8)	1450	δ <sub>a</sub> CH <sub>3</sub> (C8)	1450	δ <sub>a</sub> CH <sub>3</sub> (C8)	1450	δ <sub>a</sub> CH <sub>3</sub> (C8)	1495	δCH <sub>2</sub>
1465s	1450 m	1445	δ <sub>a</sub> CH <sub>3</sub> (C21)	1448	δCH <sub>2</sub> (C18), δCH <sub>2</sub> (C15)	1448	δ <sub>a</sub> CH <sub>3</sub> (C21)	1446	δCH <sub>2</sub> (C18)	1488	δCH <sub>2</sub>
1465s	1450 m			1443	δ <sub>a</sub> CH <sub>3</sub> (C8)	1447	δ <sub>a</sub> CH <sub>3</sub> (C8)	1442	δCH <sub>2</sub> (C12)	1469	δ <sub>s</sub> CH <sub>3</sub>
1465s	1450 m	1438	δ <sub>a</sub> CH <sub>3</sub> (C21)	1440	v <sub>a</sub> NO <sub>2</sub>	1442	δCH <sub>2</sub> (C12)	1441	δ <sub>a</sub> CH <sub>3</sub> (C8)	1450	v <sub>a</sub> NO <sub>2</sub>
1465s	1450 m	1434	δCH <sub>2</sub> (C12)	1438	δ <sub>a</sub> CH <sub>3</sub> (C21), δCH <sub>2</sub> (C12)	1437	v <sub>a</sub> NO <sub>2</sub>	1440	v <sub>a</sub> NO <sub>2</sub>	1440	v <sub>a</sub> NO <sub>2</sub>
	1417s	1429	δCH <sub>2</sub> (C18)	1435	δ <sub>a</sub> CH <sub>3</sub> (C21)	1436	δ <sub>a</sub> CH <sub>3</sub> (C21)	1436	δ <sub>a</sub> CH <sub>3</sub> (C21)		
	1417s			1428	δCH <sub>2</sub> (C18)	1432	δCH <sub>2</sub> (C15)	1430	δ <sub>a</sub> CH <sub>3</sub> (C21)	1427	wagCH <sub>2</sub>
	1417s	1422	δ <sub>a</sub> CH <sub>3</sub> (C8)	1423	δCH <sub>2</sub> (C15)	1424	δCH <sub>2</sub> (C18)				
	1417s	1414	δCH <sub>2</sub> (C15)					1417	δCH <sub>2</sub> (C15)	1416	δ <sub>s</sub> CH <sub>3</sub>
1408sh	1387 m	1396	δ <sub>s</sub> CH <sub>3</sub> (C8)	1400	δ <sub>s</sub> CH <sub>3</sub> (C8)	1402	δ <sub>s</sub> CH <sub>3</sub> (C8)	1400	ρCH <sub>2</sub> (C12), vN2–C1	1407	wagCH <sub>2</sub>
1408sh	1387 m	1391	vN2–C3	1396	vN2–C1, vN2–C3	1396	wagCH <sub>2</sub> (C15)	1399	δ <sub>a</sub> CH <sub>3</sub> (C8)	1400	wagCH <sub>2</sub>
	1387 m	1375	wagCH <sub>2</sub> (C15)	1385	wagCH <sub>2</sub> (C12)	1388	wagCH <sub>2</sub> (C12), (C15)	1387	wagCH <sub>2</sub> (C18)	1388	wagCH <sub>2</sub>
1344vs	1338 m	1363	wagCH <sub>2</sub> (C12), (C18)	1368	wagCH <sub>2</sub> (C18)			1371	wagCH <sub>2</sub> (C12)	1364	vN–C, v <sub>a</sub> NO <sub>2</sub>
1344vs	1338 m	1361	δ <sub>s</sub> CH <sub>3</sub> (C21)			1358	δ <sub>s</sub> CH <sub>3</sub> (C21)			1360	vN–C, v <sub>a</sub> NO <sub>2</sub>
1344vs	1338 m	1354	wagCH <sub>2</sub> (C12)	1353	δ <sub>s</sub> CH <sub>3</sub> (C21)	1352	wagCH <sub>2</sub> (C12)	1354	δ <sub>s</sub> CH <sub>3</sub> (C21)	1357	vN–C, v <sub>a</sub> NO <sub>2</sub>
1344vs	1338 m	1316	wagCH <sub>2</sub> (C18)	1344	vN5–C1	1340	vN2–C3	1343	vN5–C1	1348	vN–C, v <sub>a</sub> NO <sub>2</sub>
	1312sh			1312	βC1–H25, βC4–H6	1327	wagCH <sub>2</sub> (C18)	1316	wagCH <sub>2</sub> (C15)	1319	βC–H
	1302sh	1300	wagCH <sub>2</sub> (C18), (C15)	1302	vN2–C12	1312	βC1–H25	1310	ρCH <sub>2</sub> (C18)	1315	βC–H
	1302sh	1300		1302	ρCH <sub>2</sub> (C18), ρCH <sub>2</sub> (C15)	1301	τC1–H25, vN2–C12	1307	βC1–H25		
1286sh	1283sh	1292	ρCH <sub>2</sub> (C18)	1282	wagCH <sub>2</sub> (C15)	1289	ρCH <sub>2</sub> (C18)	1293	ρCH <sub>2</sub> (C18), vN5–C8	1282	ρCH <sub>2</sub>
1286sh	1283sh	1272	βC3–H7	1271	ρCH <sub>2</sub> (C18), ρCH <sub>2</sub> (C12)					1279	ρCH <sub>2</sub>
1266sh	1254w	1235	ρCH <sub>2</sub> (C15)			1257	vN27–O26, v <sub>s</sub> NO <sub>2</sub>	1249	ρCH <sub>2</sub> (C12)	1241	ρCH <sub>2</sub>
1266sh	1254w			1244	vN27–O26	1250	ρCH <sub>2</sub> (C15)	1237	ρCH <sub>2</sub> (C15)	1237	ρCH <sub>2</sub>
	1212w	1188	ρCH <sub>2</sub> (C12)	1192	ρCH <sub>2</sub> (C12)	1207	ρCH <sub>2</sub> (C12)	1197	ρCH <sub>2</sub> (C12)	1191	βC–H
1169s	1168w			1147	vN5–C8	1155	τC1–H25, τO26–H25	1139	βC1–H25, vN2–C12	1168	ρCH <sub>3</sub>
	1130sh	1134	βC1–H25	1131	ρ'CH <sub>3</sub> (C8)	1132	ρ'CH <sub>3</sub> (C8)	1132	ρ'CH <sub>3</sub> (C8)	1146	ρCH <sub>3</sub>
1119w	1117w	1118	ρ'CH <sub>3</sub> (C8)	1105	ρCH <sub>3</sub> (C21)					1121	ρCH <sub>3</sub>
1099sh	1090w	1095	βC4–H6			1094	ρCH <sub>3</sub> (C21)	1092	ρCH <sub>3</sub> (C21)	1109	ρCH <sub>3</sub>
1087sh		1087	ρCH <sub>3</sub> (C21), vC15–C18	1079	βC4–H6, βC3–H7	1081	βC3–H7, βC4–H6	1078	βC4–H6, βC3–H7	1072	v <sub>s</sub> NO <sub>2</sub>
1048w	1042vs	1075	ρ'CH <sub>3</sub> (C21)	1074	ρ'CH <sub>3</sub> (C21), τwCH <sub>2</sub> (C15)	1080	ρ'CH <sub>3</sub> (C21), ρCH <sub>3</sub> (C8)	1071	ρ'CH <sub>3</sub> (C21)	1062	vC–C
	1042vs	1069	ρCH <sub>3</sub> (C8)	1070	ρCH <sub>3</sub> (C8)	1073	ρCH <sub>3</sub> (C8)	1067	ρCH <sub>3</sub> (C8)	1040	βR <sub>2</sub>

	1042vs	1023	$\beta R_2$	1024	$\beta R_2$	1027	$\beta R_2$	1030	$\beta R_2, \nu N2-C3$	1038	$\beta R_2$
	1042vs	1013	$\beta R_1, \nu N5-C4$	1021	$\nu_3 NO_2$	1025	$\tau C1-H25, \tau O26-H25$	1021	$\nu_3 NO_2, \nu N27-O26$	1032	$\beta R_1$
1028w	1023 m			1017	$\nu C15-C18, \nu C18-C21$	1017	$\gamma C1-H25$			1031	$\beta R_1$
1028w	1023 m	1003	$\nu C18-C21$			1014	$\tau C1-H25, \tau O26-H25$	1011	$\nu C18-C21$		
	988vw			998	$\beta R_1, \nu N5-C4$	999	$\nu N5-C4, \beta R_1$	999	$\beta R_1, \nu N5-C4$	999	$\beta R_1, \nu C-C$
	988vw			992	$\gamma C1-H25$			993	$\gamma C1-H25$	993	$\nu C-C$
982vw	974w			976	$\nu C12-C15$	962	$\nu C12-C15, \nu C18-C21$			989	$\gamma C-H$
952vw	947w	957	$\nu C12-C15$					959	$\nu C12-C15$	957	$\tau w CH_2$
897sh	906w	908	$\rho CH_3(C21)$	893	$\tau w CH_2(C12), \rho' CH_3(C21)$	910	$\tau w CH_2(C12)$	911	$\tau w CH_2(C12)$	921	$\gamma C-H$
	883w			888	$\rho CH_3(C21), \nu C15-C18$					891	$\tau w CH_2$
862sh	860vw	867	$\gamma_a C-H$							858	$\gamma C-H$
862sh	860vw	842	$\tau w CH_2(C15)$			847	$\tau w CH_2(C15), \rho' CH_3(C21)$	844	$\tau w CH_2(C15)$		
837 m	826w	821	$\gamma C1-H25$	838	$\gamma_a C-H$	840	$\gamma_a C-H$	839	$\gamma_a C-H$	836	$\gamma NO_2$
825sh	811w			814	$\gamma NO_2$	817	$\gamma NO_2$	814	$\gamma NO_2$	828	$\gamma NO_2$
761 m		774	$\tau w CH_2(C12), \nu C15-C18$			776	$\tau w CH_2(C12), \nu C15-C18$	778	$\nu C15-C18$	764	$\tau w CH_2$
743sh	752w	741	$\gamma s C-H$	740	$\tau w CH_2(C18)$					760	$\tau w CH_2$
731sh	733w			727	$\gamma s C-H$	729	$\gamma s C-H$	727	$\gamma s C-H$	745	$\gamma C-H$
731sh	733w			721	$\nu N2-C12$					720	$\delta NO_2$
	711sh	701	$\tau w CH_2(C18)$			712	$\rho NO_2$			717	$\delta NO_2$
702w	706w			710	$\rho NO_2$	710	$\rho NO_2$	710	$\rho NO_2$	716	$\delta NO_2$
							$\tau w CH_2(C18)$				
702w	706w			706	$\delta NO_2$	707	$\delta NO_2$	706	$\delta NO_2$	715	$\delta NO_2$
	699sh							702	$\tau w CH_2(C18)$	706	$\nu N-C$
672sh		668	$\nu N5-C8$	669	$\tau w CH_2(C15)$	673	$\tau w CH_2(C18), \nu N5-C8$	673	$\nu N5-C8$	672	$\tau R_1$
658w	658w			650	$\gamma N2-C12$					663	$\tau R_1$
624 m	624w	634	$\tau R_1$			636	$\tau C1-H25, \tau R_1$	636	$\tau R_1$	641	$\tau R_1$
604w	601w	613	$\tau R_2$	618	$\tau R_2$	615	$\tau R_2, \tau R_1$	615	$\tau R_2$	635	$\tau R_2$
604w	601w			610	$\tau R_1$					600	$\tau R_2$
604w	601w	570	$\nu N2-C12$			578	$\nu N2-C12$	581	$\nu N2-C12$	592	$\tau R_2$
	500w	481	$\delta_c 12C15C18$	432	$\delta_c 15C18C21, \delta N2C12C15$	501	$\delta_c 15C18C21$	486	$\delta_c 12C15C18$	499	$\delta CCC$
	415w	410	$\beta N5-C8, \beta N2-C12$	409	$\beta N2-C12$	413	$\beta N5-C8$	417	$\beta N5-C8, \beta N2-C12$	420	$\beta N-C$
	326w	320	$\delta N2C12C15$	315	$\nu N2-C12$	318	$\delta N2C12C15$	311	$\delta_c 15C18C21, \delta N2C12C15$	331	$\delta CCC, \delta NCC$
	285vw	282	$\delta_c 15C18C21$	281	$\beta N5-C8$	294	$\beta N2-C12, \gamma N2-C12$	299	$\beta N5-C8, \beta N2-C12$	294	$\beta N-C$
	258vw	241	$\gamma N5-C8$	244	$\gamma N5-C8, \delta_c 12C15C18$	251	$\gamma N5-C8$	241	$\gamma N5-C8$	253	$\gamma N-C$
	215sh	221	$\tau w CH_3(C21)$	210	$\tau w CH_3(C21)$	223	$\tau w CH_3(C21)$	219	$\tau w CH_3(C21), \gamma N5-C8$	219	$\gamma N-C$
	198sh	201	$\delta_c 12C15C18, \gamma N5-C8$	195	$\gamma N5-C8, \delta_c 12C15C18$	199	$\delta_c 12C15C18$	204	$\tau w CH_3(C21)$	204	$\tau w CH_3$
	198sh					176	$\tau C1-H25, \tau O26-H25$			175	$\tau C-C$
				163	$\nu H25-O26$	164	$\nu H25-O26$	157	$\nu H25-O26$	162	$\tau w CH_3$
		141	$\gamma N2-C12$			145	$\tau w CH_3(C8)$	154	$\gamma N2-C12$	149	$\tau w CH_3$
				136	$\tau w CH_3(C8)$			134	$\tau w CH_3(C8)$	142	$\tau w CH_3$
	110s			105	$\tau C15-C18$	113	$\delta_H 25O26N27, \delta_c 1H25O26$			125	$\delta CH_3, \delta HON$
	110s			100	$\delta_H 25O26N27$			95	$\delta_H 25O26N27$	104	$\delta HON$
	84sh			82	$\tau C1-H25$	86	$\tau C1-H25, \tau O26-H25$			86	$\tau C-C$
	84sh	75	$\tau C15-C18, \tau C12-C15$					78	$\tau C15-C18, \tau C12-C15$	78	$\tau N-O$
		66	$\gamma N5-C8$	74	$\tau C12-C15$	70	$\tau C12-C15, \tau C15-C18$	70	$\tau C1-H25$	72	$\tau N-O$
				69	$\tau C1-H25$						
		58	$\tau w CH_3(C8)$	56	$\tau N27-O26$	60	$\delta_H 25O26N27, \delta_c 1H25O26$	60	$\delta_H 25O26N27, \delta_c 1H25O26$	60	$\tau C-H$
				50	$\delta_H 25O26N27, \tau C1-H25$	45	$\tau C1-H25, \tau O26-H25$	46	$\delta_H 25O26N27, \delta_c 1H25O26$	48	$\tau C-H$
						33	$\tau w C12-N2$	31	$\tau N27-O26, \tau w C12-N2$	37	$\tau w C-N$
				26	$\tau C1-H25, \tau O26-H25$	28	$\tau N27-O26$	23	$\delta_c 1H25O26$	28	$\tau w C-N$
		19	$\tau w C12-N2$	17	$\delta_c 1H25O26$			14	$\tau O26-H25$	20	$\tau O-H$
				11	$\tau O26-H25$	9	$\tau O26-H25$			13	$\tau O-H$
RMSD (cm <sup>-1</sup> )	24.14			19.73		19.01		18.03			

Abbreviations: v, stretching; wag, wagging;  $\tau$ , torsion;  $\rho$ , rocking;  $\tau w$ , twisting;  $\delta$ , deformation; a, antisymmetric; s, symmetric.

<sup>a</sup> This work.

<sup>b</sup> From Ref [17].

<sup>c</sup> From scaled quantum mechanics force field B3LYP/6-311++G\*\* method.

<sup>d</sup> From B3LYP/6-311++G\*\* method.

**Table 10**  
Comparison of scaled internal force constants for the most stable conformers of 1-buthyl-3-methyl imidazolium nitrate and their cation in gas phase.

B3LYP Method						
Force constants	6-31G** <sup>a</sup>			6-311++G**		6-311++G
	1-buthyl-3-methyl imidazolium		1-buthyl-3-methyl imidazolium nitrate		p-xylylene-diaminium bis(nitrate) <sup>b</sup>	Chromyl nitrate <sup>c</sup>
	Cation		C1	C2	C3	
$f(\nu N=O)$		8.50	8.30	8.30	9.74	15.83
$f(\nu N-O)$		6.80	6.90	6.90	4.25	3.22
$f(\nu C-H)$	5.50	5.16	5.23	5.20		
$f(\nu CH_2)$	4.80	4.78	4.78	4.81		
$f(\nu CH_3)$	4.97	4.88	4.88	4.90		
$f(\nu C-N)_R$	6.75	6.75	6.82	6.75		
$f(\nu C-N)$	4.25	4.45	4.50	4.50		
$f(\nu C=C)$	7.70	7.80	7.80	7.80		
$f(\nu C-C)$	4.00	4.03	4.03	4.03		
$f(\delta CH_2)$	0.80	0.80	0.80	0.80		
$f(\delta CH_3)$	0.57	0.60	0.58	0.55		
$f(\delta NO_2)$		1.60	1.60	1.60	1.53	
B3LYP Method						
Force constants	6-311++G** <sup>a</sup>			6-311++G**		6-311++G
	1-buthyl-3-methyl imidazolium		1-buthyl-3-methyl imidazolium nitrate		p-xylylene-diaminium bis(nitrate) <sup>b</sup>	Chromyl nitrate <sup>c</sup>
	Cation		C1	C2	C3	
$f(\nu N=O)$		8.00	8.00	7.95	9.74	15.83
$f(\nu N-O)$		6.50	6.50	6.50	4.25	3.22
$f(\nu C-H)$	5.40	5.10	5.14	5.13		
$f(\nu CH_2)$	4.73	4.73	4.71	4.73		
$f(\nu CH_3)$	4.87	4.82	4.80	4.82		
$f(\nu C-N)_R$	6.60	6.57	6.60	6.60		
$f(\nu C-N)$	4.15	4.35	4.35	4.35		
$f(\nu C=C)$	7.60	7.60	7.60	7.60		
$f(\nu C-C)$	3.93	3.93	3.93	3.93		
$f(\delta CH_2)$	0.77	0.8	0.80	0.80		
$f(\delta CH_3)$	0.52	0.52	0.53	0.52		
$f(\delta NO_2)$		1.60	1.60	1.60	1.53	

Units are  $\text{mdyn \AA}^{-1}$  for stretching and  $\text{mdyn \AA rad}^{-2}$  for angle deformations.

<sup>a</sup> This work.

<sup>b</sup> From Ref. [34].

<sup>c</sup> From Ref. [41,42].

in the three conformers they are predicted between 1450 and 1396  $\text{cm}^{-1}$  and, for this reason, those modes were clearly assigned in this region, as detailed in Table 9. The symmetric  $\text{CH}_3$  deformation mode predicted in the dimer at 1416  $\text{cm}^{-1}$  can be easily assigned to the strong Raman band at 1417  $\text{cm}^{-1}$ . The rocking modes are predicted in different regions and in some cases coupled with other modes, thus, in the cation they are predicted between 1118 and 908  $\text{cm}^{-1}$ , in the three conformers between 1132 and 847  $\text{cm}^{-1}$  while in the dimer between 1168 and 1109  $\text{cm}^{-1}$ . Hence, the bands observed in those regions are assigned to these vibration modes.

The twisting modes are predicted for all species in approximately the same regions, and in particular, in C3 one of them is predicted coupled with the out-of-plane deformation mode. In the cation, these modes are predicted in 221 and 58  $\text{cm}^{-1}$  while in the monomers between 223 and 134  $\text{cm}^{-1}$ , as in species with similar groups [26,36,39]. In the dimer these modes are predicted between 204 and 142  $\text{cm}^{-1}$ , as indicated in Table 9.

### 5.1.3. $\text{CH}_2$ modes

The antisymmetric and symmetric stretching modes expected for the three  $\text{CH}_2$  groups of cation and the three conformers of  $[\text{BMIm}][\text{NO}_3]$  are predicted between 2993 and 2872  $\text{cm}^{-1}$  while in the dimer, they are predicted between 3003 and 2998  $\text{cm}^{-1}$ , hence, the IR and Raman bands observed in these regions can be assigned to those vibration modes. Note that the symmetric modes were

assigned to the Raman bands of medium intensities at 2962, 2941, 2913 and 2874  $\text{cm}^{-1}$ , as observed for other species containing these groups [26,27,36,39]. The deformation, wagging, rocking and twisting modes expected for these species were predicted in the expected regions [26,27,36,39] and for this reason, they were assigned to the IR and Raman bands at 1450/1417, 1417/1283, 1302/1112 and 952/672  $\text{cm}^{-1}$ , respectively.

### 5.1.4. Nitrate groups

Here, the nitrate groups in the three monomers and dimer of  $[\text{BMIm}][\text{NO}_3]$  were considered with monodentate coordinations because the N–O bonds were predicted by SQM calculations with different values (see Table 2) because one of the tree bonds is predicted with lower value (N–O) than the other ones ( $\text{O}=\text{N}=\text{O}$ ), as observed in similar nitrate species [35,40–43]. For instance, the N=O stretching modes are observed between 1672 and 1460  $\text{cm}^{-1}$  [40–42] but, in  $\text{NbO}(\text{NO}_3)_3$  these modes were assigned between 1763 and 1753  $\text{cm}^{-1}$  [43]. Considering bidentate coordination in p-xylylenediaminiumbis(nitrate) [34], the  $\text{NO}_2$  antisymmetric stretching modes were assigned at 1313  $\text{cm}^{-1}$  while the N=O stretching modes were assigned at 1536  $\text{cm}^{-1}$ . Here, we expected for the nitrate groups of monomers two  $\text{NO}_2$  antisymmetric and symmetric stretching modes and only one N–O stretching mode. The strong IR band at 1465  $\text{cm}^{-1}$  is clearly assigned to the  $\text{NO}_2$  antisymmetric stretching modes for the three monomers while in the dimer these modes are assigned to the strong IR band at

1344  $\text{cm}^{-1}$ . However, the corresponding symmetric modes are predicted in different regions in the three species, thus, these modes in C1 and C3 are assigned to the very strong Raman band at 1042  $\text{cm}^{-1}$  while in C2 that symmetric mode is predicted at 1257  $\text{cm}^{-1}$  coupled with the N27–O26 stretching mode. In the dimer the symmetric stretching mode is predicted at 1072  $\text{cm}^{-1}$  but assigned to the strong Raman band at 1042  $\text{cm}^{-1}$ . In p-xylylene-diaminiumbis(nitrate) [34] the deformation modes were predicted by calculations at 783  $\text{cm}^{-1}$  while the two O=N=O deformation modes in the monomers and dimer species are predicted between 720 and 706  $\text{cm}^{-1}$ . Here, these deformation modes were assigned to the Raman bands between 733 and 706  $\text{cm}^{-1}$  while the rocking modes were also assigned to the shoulder at 711  $\text{cm}^{-1}$  because these modes are predicted in this region. The wagging modes were assigned to the weak Raman bands at 826 and 811  $\text{cm}^{-1}$  because they are predicted by calculations at 836/814  $\text{cm}^{-1}$ . The torsion modes were assigned as predicted by calculations at 78/28  $\text{cm}^{-1}$ , as detailed in Table 9.

### 5.1.5. Skeletal modes

The N5=C1, N2=C1 and C3=C4 stretching modes were predicted in the three conformers and the cation in different regions, and, for these reasons, these bonds present different double bond characteristics, as observed in Table 9. Thus, in the cation, these modes are predicted at 1548 (N5=C1, C3=C4) and 1539 (N2=C1)  $\text{cm}^{-1}$  and with double bond characters while in C1 are predicted at 1550 (C3=C4), 1396 (N2=C1) and 1344 (N5=C1)  $\text{cm}^{-1}$ , where clearly only the two latter have partial double bond character. In C2, the three bonds have double bond characters because they are predicted at 1550 and 1539  $\text{cm}^{-1}$  while in C3, the C3=C4 and N2=C1 stretching modes are predicted with double bond characters at 1550 and 1533  $\text{cm}^{-1}$  while the N5=C1 stretching mode is predicted with partial double bond character because it is predicted at 1343  $\text{cm}^{-1}$ . Evidently, the presence of the anion and the position of the side chain modify in part the nature and characteristics of these bonds. The N5–C8 stretching modes, in species containing the N–CH<sub>3</sub> group, such as tropane species, are predicted at 1128–1031  $\text{cm}^{-1}$  [44–46]. Here, the N5–CH<sub>3</sub> stretching modes of the four species are predicted in different regions, hence, in C1 is predicted at 1147  $\text{cm}^{-1}$  while in the cation, C2 and C3 are predicted between 673 and 668  $\text{cm}^{-1}$ . The other N2–C12 bonds are linked to the butyl groups, as it is expected due to their longer chain in the lower wavenumbers region. Thus, in the cation that mode is predicted at 570  $\text{cm}^{-1}$ , in C1 at 315  $\text{cm}^{-1}$ , in C2 at 578  $\text{cm}^{-1}$  while in C3 at 581  $\text{cm}^{-1}$ . Later, they were assigned in these regions, as can be observed in Table 9. The C–C stretching modes corresponding to the butyl chain are predicted with simple bond characters, as it is expected and, for this reason, they are assigned between 1017 and 778  $\text{cm}^{-1}$ , as predicted by calculations. The two expected deformations ( $\beta_{R1}$  and  $\beta_{R2}$ ) and torsions ( $\tau_{R1}$  and  $\tau_{R2}$ ) rings, for the imidazoline rings were assigned as predicted the SQM calculations and, as reported for similar species with five members rings [44–46].

## 6. Force constants

In Table 10, for the three conformers of [BMIm][NO<sub>3</sub>] and their [BMIm] cation, the calculated force constants are presented compared with those reported for p-xylylene-diaminium bis(nitrate) [34] and chromyl nitrate [41,42]. They were computed from their corresponding harmonic force fields calculated at by the using 6-31G\* and 6-311++G\*\* basis sets and with the SQMFF methodology [22] and the Molvib program [23]. Analyzing the force constants values for the three conformers at by the using 6-31G\* basis set we observed that the  $f(\nu N=O)$  and  $f(\nu N-O)$  constant values

practically do not change in C2 and C3 but in C1 the values are slightly different from C2 and C3. On the other hand, the  $f(\nu C-N)_R$  and  $f(\nu C-N)$  force constants related to the rings and to the side chains are completely different, as it is expected because the bonds related with these constants that belong to the rings present double bonds characters and, for this reason, they have higher values than the other ones. And, for the same reason, the  $f(\nu C=C)$  and  $f(\nu C-C)$  force constants present different values. When the other basis set is used the values undergo clear diminishing with exception of the  $f(\delta CH_2)$  and  $f(\delta NO_2)$  force constants probably because their corresponding bond angles do not change when the size of the basis set increases. When the values for the  $f(\nu N=O)$  and  $f(\nu N-O)$  constants are compared with those reported for p-xylylene-diaminium bis(nitrate) [34] and for chromyl nitrate [41,42] we observed different values. In the first case, probably the observed differences can be justified by the two nitrate groups present in p-xylylene-diaminium bis(nitrate) [34] while in the second case the presence of strong bidentate coordinations with the Cr atom can explain those differences observed.

## 7. Conclusions

In the present work, we have studied the cation-anion interactions of the 1-butyl-3-methylimidazolium nitrate ionic liquid in gas phase by using the hybrid B3LYP/6-31G\* and B3LYP/6-311++G\*\* calculations and the experimental Raman spectrum. From the four C1, C2, C3 and C4 conformers found in the PES for this ionic liquid, by using both levels of theory, only three of them were studied because C2 and C4 have practically the same energies and properties. The results obtained for C1, C2 and C3 show better correlations in geometries and wavenumbers when the 6-311++G\*\* basis set is employed, as evidenced by their corresponding RMSD values. Here, the atomic charges, molecular electrostatic potentials, stabilization energies, bond orders and topological properties were computed for those three most stable isomers. The MK charges suggest coordination monodentate for the three conformers while the studies by means of the Mulliken charges, MEPs and BO clearly support the coordination bidentate for the nitrate groups of [BMIm][NO<sub>3</sub>]. Besides, the total sum of the MK charges on the C1, N2 and N5 atoms evidence positive sign on the imidazole ring, a result different from that obtained for the Mulliken ones. The NBO study shows clear differences among the three conformers being the more stable C1 by using 6-31G\* basis set and C2 with the other basis set. Besides, the NBO study evidences high stability of the neutral species as compared with the cation. Evidently, the nitrate groups strongly stabilize the [BMIm] cation in the ionic liquid. The AIM study reveals the high stability of the C2 conformer of [BMIm][NO<sub>3</sub>] and clearly supports the bidentate coordination for their three conformers. Both NBO and AIM calculations support the high stability of C2 by using the B3LYP/6-311++G\*\* level of theory. The SQMFF procedure was employed together with the normal internal coordinates and the experimental available FTIR and FTRaman in order to perform the complete vibrational assignments of all species. The force constants were also reported for the monomers and their cation by using both levels of theory. The presence of the dimeric species of ionic liquid supports the strong bands observed in both experimental infrared and Raman spectra at 1344 and 1042  $\text{cm}^{-1}$ , respectively. The study by the frontier orbitals reveals that the ionic liquid is slightly less reactive than the cation probably due to the low values of nucleophilicity and electrophilicity indexes of the ionic liquid. Finally, the reactivities and behaviour of these species in gas phase slightly change when the size of the basis set increases.

## Acknowledgements

This work was supported with grants from CIUNT Project N° 26/ D207 (Consejo de Investigaciones, Universidad Nacional de Tucumán). The authors would like to thank Prof. Tom Sundius for his permission to use MOLVIB.

## Appendix A. Supplementary data

Supplementary data related to this article can be found at <https://doi.org/10.1016/j.molstruc.2018.03.100>.

## References

- [1] G. Gonfa, M.A. Bustam, Z. Man, M.I. Abdul Mutalib, Unique structure and solute-solvent interaction in imidazolium based ionic liquids: a review, *Asian Trans. Eng.* 1 (5) (2011) 24–34 (ATE-20114053).
- [2] H. Weingärtner, Understanding ionic liquids at the molecular level: facts, problems, and controversies, *Angew. Chem. Int. Ed.* 47 (2008) 654–670.
- [3] V. Bennett, S.S. Angaye, E.D. Dikio, Conductance of 1-Butyl-3-methylimidazolium nitrate [BMim][NO<sub>3</sub>] with N,N-dimethylformamide at T (293.15 – 323.15) K, *Int. J. Chem. Chem. Proc.* 3 (1) (2017) 23–34.
- [4] S. Ivanova, L.F. Bobadilla, A. Penkova, F. Romero Sarria, M.A. Centeno, J.A. Odriozola, Gold functionalized supported ionic liquids catalyst for CO oxidation, *Catalysts* 1 (2011) 52–68.
- [5] K.I. Seethalakshmi, E. Jasmine Vasantha Rani, R.1 Padmavathy, N. Radha, FT-IR spectral analysis of imidazolium chloride, *Int. J. Cur. Res. Rev.* 4 (19) (2012) 31–36.
- [6] L.N. Sim, S.R. Majid, A.K. Arof, Effects of 1-butyl-3-methyl imidazolium trifluoromethanesulfonate ionic liquid in poly(ethyl methacrylate)/poly(vinylidene fluoride-co-hexafluoropropylene) blend based polymer electrolyte system, *Electrochim. Acta* 123 (2014) 190–197.
- [7] Takahiro Takekiyo, Yukihiko Yoshimura, Ionic liquid-induced unique structural transitions of proteins, progress and developments in ionic liquids, *Intech, Chapter 5* (2017) 97–116, <https://doi.org/10.5772/65886>.
- [8] Hiranmayee Kandala, Comprehensive Structural, Thermal and Toxicological Characterization of 1-ethyl-3-methylimidazolium Alkylbenzenesulfonate Ionic Liquids, Thesis, South Dakota State University, 2017.
- [9] Jingsi Gao, Norman J. Wagner, A new correlation between excess viscosity and excess molar volume for 1-butyl-3-methylimidazolium tetrafluoroborate ([C4mim][BF<sub>4</sub>]) mixtures with water, *Langmuir, J. Mol. Liq.* 223 (2016) 678–686.
- [10] Alexander Kokorin (Ed.), *Ionic liquids: Applications and Perspectives*, Intech, 2011.
- [11] Mukund Ghavre, Low Toxicity Imidazolium & Pyridinium Ionic Liquids: Synthesis, Antimicrobial Toxicity, Biodegradation Studies and Applications in Tsuji-trost Reactions, Thesis, School of Chemical Sciences Dublin City University, 2012.
- [12] M. Keyler, Nanocatalysis in Ionic Liquids Syntheses, Characterisation and Application of Nanoscale Catalysts, Thesis, Universität zu Köln, 2014.
- [13] C. Aliaga, S. Baldelli, Sum frequency generation spectroscopy and double-layer capacitance studies of the 1-butyl-3-methylimidazolium dicyanamide-platinum interface, *J. Phys. Chem. B* 110 (37) (2006) 18481–18491.
- [14] J.-H. Wang, D.-H. Cheng, X.-W. Chen, Z. Du, Z.-L. Fang, Direct extraction of double-stranded DNA into ionic liquid 1-Butyl-3-methylimidazolium hexafluorophosphate and its quantification, *Anal. Chem.* 79 (2) (2007) 620–625.
- [15] M.-A. Neouze, M. Litschauer, Confinement of 1-Butyl-3-methylimidazolium nitrate in metallic silver, *J. Phys. Chem. B* 112 (51) (2008) 16721–16725.
- [16] P.A. Hunt, I.R. Gould, Structural characterization of the 1-Butyl-3-methylimidazolium chloride ion pair using ab initio methods, *J. Phys. Chem.* 110 (6) (2006) 2269–2282.
- [17] M.S. Gruzdev, L.M. Ramenskaya, U.V. Chervonova, R.S. Kumeev, Preparation of 1-butyl-3-methylimidazolium salts and study of their phase behavior and intra-molecular interactions, *Russ. J. Gen. Chem.* 79 (8) (2009) 1720–1727.
- [18] E.P. Grishina, et al., Water effect on physicochemical properties of 1-butyl-3-methylimidazolium based ionic liquids with inorganic anions, *J. Mol. Liq.* 177 (2013) 267–272.
- [19] E.D. Glendening, J.K. Badenhop, A.D. Reed, J.E. Carpenter, F. Weinhold, NBO 3.1, Theoretical Chemistry Institute, University of Wisconsin, Madison, WI, 1996.
- [20] F. Biegler-König, J. Schönbohm, D. Bayles, AIM2000; a program to analyze and visualize atoms in molecules, *J. Comput. Chem.* 22 (2001) 545.
- [21] R.F.W. Bader, *Atoms in Molecules, A Quantum Theory*, Oxford University Press, Oxford, 1990, ISBN 0198558651.
- [22] a) G. Rauhut, P. Pulay, *J. Phys. Chem.* 99 (1995) 3093–3099; b) Correction G. Rauhut, P. Pulay, *J. Phys. Chem.* 99 (1995) 14572.
- [23] T. Sundius, Scaling of ab initio force fields by MOLVIB, *Vib. Spectrosc.* 29 (2002) 89–95.
- [24] R.G. Parr, R.G. Pearson, Absolute hardness: companion parameter to absolute electronegativity, *J. Am. Chem. Soc.* 105 (1983) 7512–7516.
- [25] J.-L. Brédas, Mind the gap!, *Materials Horizons* 1 (2014) 17–19.
- [26] F. Chain, M.A. Iramain, A. Grau, C.A.N. Catalán, S.A. Brandán, Evaluation of the structural, electronic, topological and vibrational properties of N-(3,4-dimethoxybenzyl)-hexadecanamide isolated from Maca (*Lepidium meyenii*) using different spectroscopic techniques, *J. Mol. Struct.* 1119 (2016) 25–38.
- [27] D. Romani, S.A. Brandán, M.J. Márquez, M.B. Márquez, Structural, topological and vibrational properties of an isothiazole derivatives series with antiviral activities, *J. Mol. Struct.* 1100 (2015) 279–289.
- [28] D. Romani, S. Tsuchiya, M. Yotsu-Yamashita, S.A. Brandán, Spectroscopic and structural investigation on intermediates species structurally associated to the tricyclic biguanidine compound and to the toxic agent, saxitoxin, *J. Mol. Struct.* 1119 (2016) 25–38.
- [29] A.B. Nielsen, A.J. Holder, *Gauss View 3.0, User's Reference*, GAUSSIAN INC., Pittsburgh, PA, 2000–2003.
- [30] M.J. Frisch, G.W. Trucks, H.B. Schlegel, G.E. Scuseria, M.A. Robb, J.R. Cheeseman, G. Scalmani, V. Barone, B. Mennucci, G.A. Petersson, H. Nakatsuji, M. Caricato, X. Li, H.P. Hratchian, A.F. Izmaylov, J. Bloino, G. Zheng, J.L. Sonnenberg, M. Hada, M. Ehara, K. Toyota, R. Fukuda, J. Hasegawa, M. Ishida, T. Nakajima, Y. Honda, O. Kitao, H. Nakai, T. Vreven, J.A. Montgomery Jr., J.E. Peralta, F. Ogliaro, M. Bearpark, J.J. Heyd, E. Brothers, K.N. Kudin, V.N. Staroverov, R. Kobayashi, J. Normand, K. Raghavachari, A. Rendell, J.C. Burant, S.S. Iyengar, J. Tomasi, M. Cossi, N. Rega, J.M. Millam, M. Klene, J.E. Knox, J.B. Cross, V. Bakken, C. Adamo, J. Jaramillo, R. Gomperts, R.E. Stratmann, O. Yazyev, A.J. Austin, R. Cammi, C. Pomelli, J.W. Ochterski, R.L. Martin, K. Morokuma, V.G. Zakrzewski, G.A. Voth, P. Salvador, J.J. Dannenberg, S. Dapprich, A.D. Daniels, O. Farkas, J.B. Foresman, J.V. Ortiz, J. Cioslowski, D.J. Fox, *Gaussian 09, Revision A.02*, Gaussian, Inc., Wallingford CT, 2009.
- [31] H. Geng, L-h Zhuang, J. Zhang, G-w. Wang, A-I Yuan, 3,3-Dimethyl-1,1-(butane-1,4-diyl)-diimidazolium bis(tetrafluoroborate), *Acta Crystallogr. E66* (2010) o1267.
- [32] B.H. Besler, K.M. Merz Jr., P.A. Kollman, Atomic charges derived from semi-empirical methods, *J. Comp. Chem.* 11 (1990) 431–439.
- [33] P. Ugliengo, *MOLDRAW Program*, University of Torino, Dipartimento Chimica IFM, Torino, Italy, 1998.
- [34] S. Gatfaoui, N. Issaoui, S.A. Brandán, T. Roisnel, H. Marouani, Synthesis and characterization of p-xylylenediaminiumbis(nitrate). Effects of the coordination modes of nitrate groups on their structural and vibrational properties, *J. Mol. Struct.* 1135 (2017) 209–221.
- [35] D. Romani, S.A. Brandán, Structural, electronic and vibrational studies of two 1,3-benzothiazole tautomers with potential antimicrobial activity in aqueous and organic solvents. Prediction of their reactivities, *Computational and Theoretical Chem.* 1061 (2015) 89–99.
- [36] M.B. Márquez, S.A. Brandán, A structural and vibrational investigation on the antiviral deoxyribonucleoside thymidine agent in gas and aqueous solution phases, *Int. J. Quant. Chem.* 114 (2014) 209–221.
- [37] G. Keresztury, S. Holly, G. Besenyi, J. Varga, A.Y. Wang, J.R. Durig, Vibrational spectra of monothiocarbamates-II. IR and Raman spectra, vibrational assignment, conformational analysis and ab initio calculations of S-methyl-N,N-dimethylthiocarbamate, *Spectrochim. Acta* 49A (1993) 2007–2026.
- [38] D. Michalska, R. Wysokinski, The prediction of Raman spectra of platinum(II) anticancer drugs by density functional theory, *Chem. Phys. Lett.* 403 (2005) 211–217.
- [39] F.E. Chain, M.F. Ladetto, A. Grau, C.A.N. Catalán, S.A. Brandán, Structural, electronic, topological and vibrational properties of a series of N-benzylamides derived from Maca (*Lepidium meyenii*) combining spectroscopic studies with ONION calculations, *J. Mol. Struct.* 1105 (2016) 403–414.
- [40] ISBN: 978-1-62257-352-3, Edited Collection S.A. Brandán (Ed.), Nitrate: Occurrence, Characteristics and Health Considerations, Nova Science Publishers, Inc, 2012.
- [41] S.A. Brandán, in: Ken Derham (Ed.), A structural and vibrational study of the chromyl chlorosulfate, fluorosulfate, and nitrate compounds, vol. 1, Springer Science, Business Media B.V., Van Godewijkstraat 30, 3311 GZ Dordrecht, Netherlands, 2012. ISBN: 978-94-007-5762-2.
- [42] S.A. Brandán (Ed.), *Descriptors, Structural and Spectroscopic Properties of Heterocyclic Derivatives of Importance for the Health and the Environmental*, Edited Collection, Nova Science Publishers, Inc, 2015. ISBN: 978-1-63482-708-9.
- [43] M.V. Castillo, E. Romano, H.E. Lanús, S.B. Díaz, A. Ben Altobelli, S.A. Brandán, Theoretical structural and experimental vibrational study of niobyl nitrate, *J. Mol. Struct.* 994 (2011) 202–208.
- [44] S.A. Brandán, Why morphine is a molecule chemically powerful. Their comparison with cocaine, *Indian J. Appl. Res.* 7 (7) (2017) 511–528.
- [45] R.A. Rudyk, S.A. Brandán, Force field, internal coordinates and vibrational study of alkaloid tropane hydrochloride by using their infrared spectrum and DFT calculations, *Paripex Indian J. Res.* 6 (8) (2017) 616–623.
- [46] D. Romani, S.A. Brandán, Vibrational analyses of alkaloid cocaine as free base, cationic and hydrochloride species based on their internal coordinates and force fields, *Paripex Indian J. Res.* 6 (9) (2017) 587–602.